Warsaw February 29,2012

Nuclear Physics results that worry me

Kirby Kemper Florida State University

Map of Florida

Florida State University in 1851-First as a seminary for men then in 1904 as a women's college and then in 1947 became a co-ed university.

Today has 39,000 students.

Accelerator Laboratory at Florida State

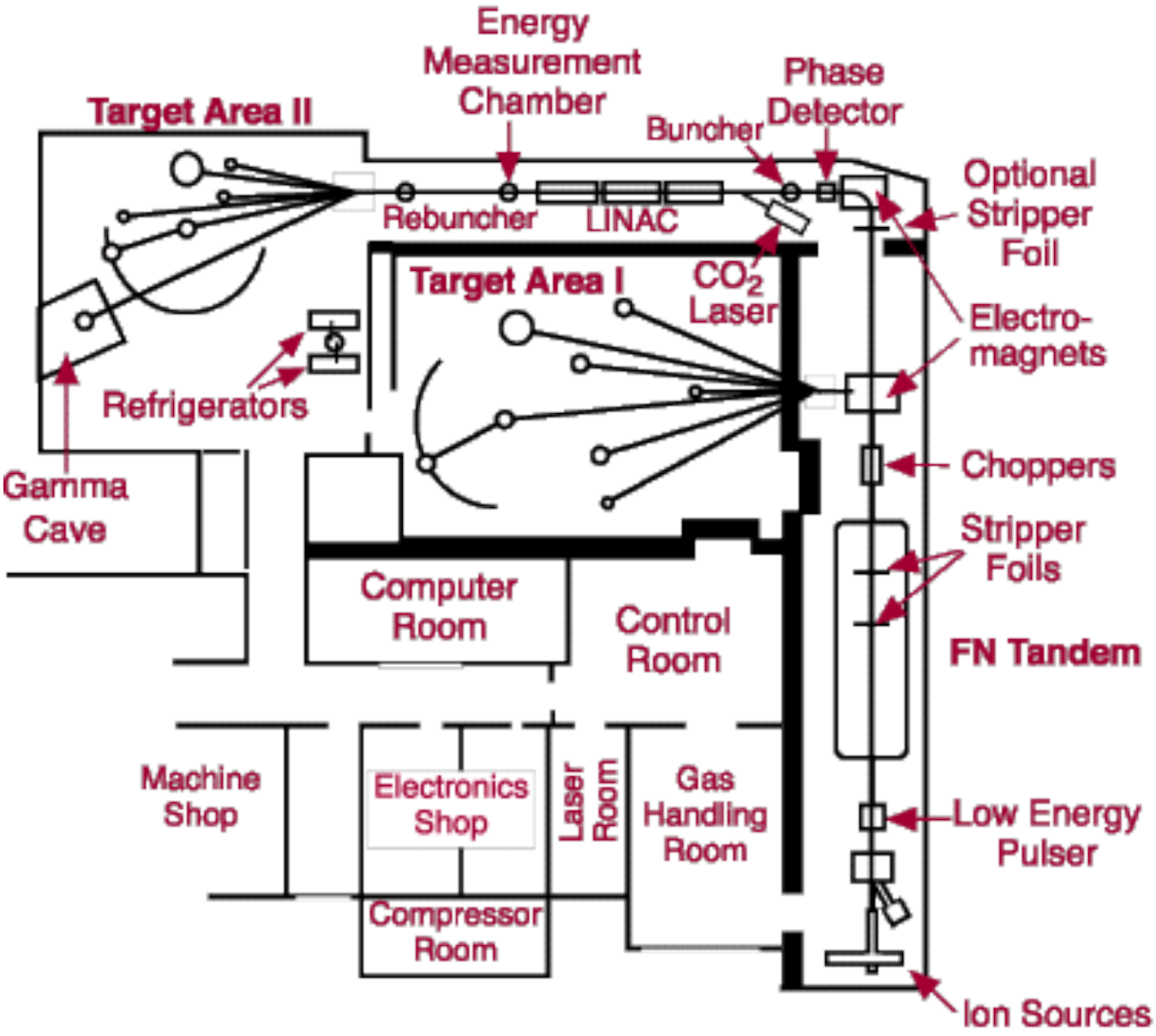

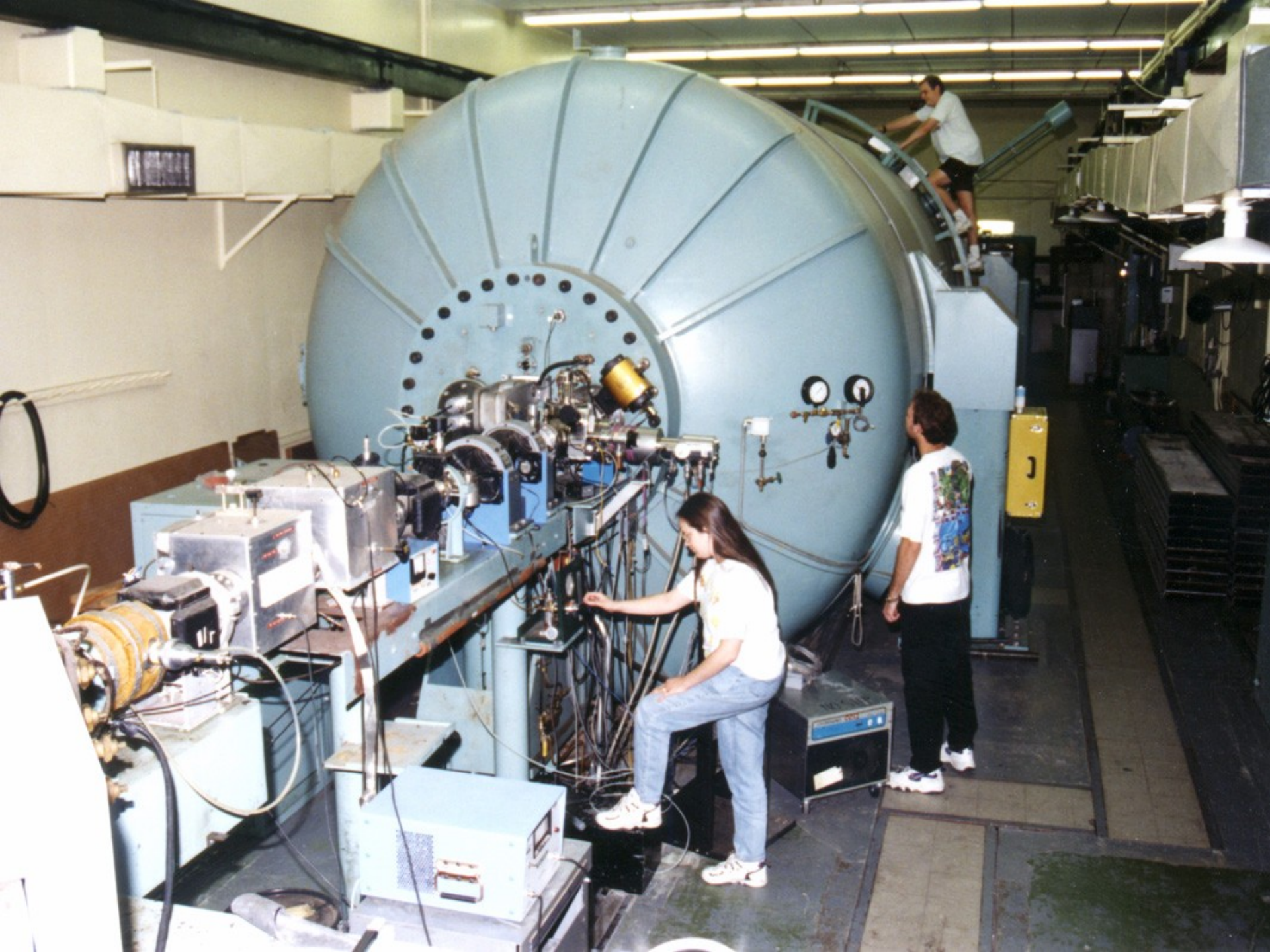

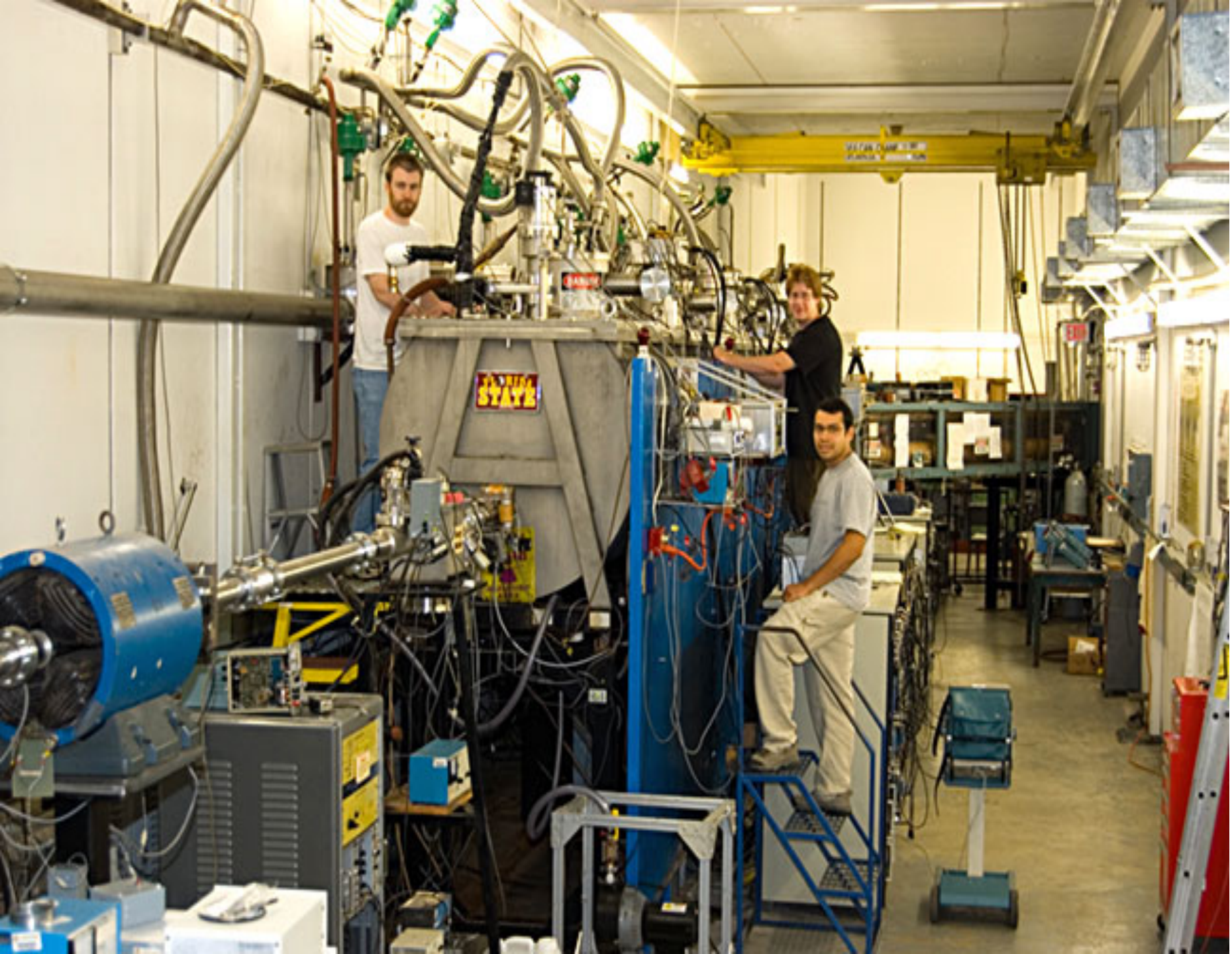
STATE

RESOLUT: a new radioactive beam facility at FSU

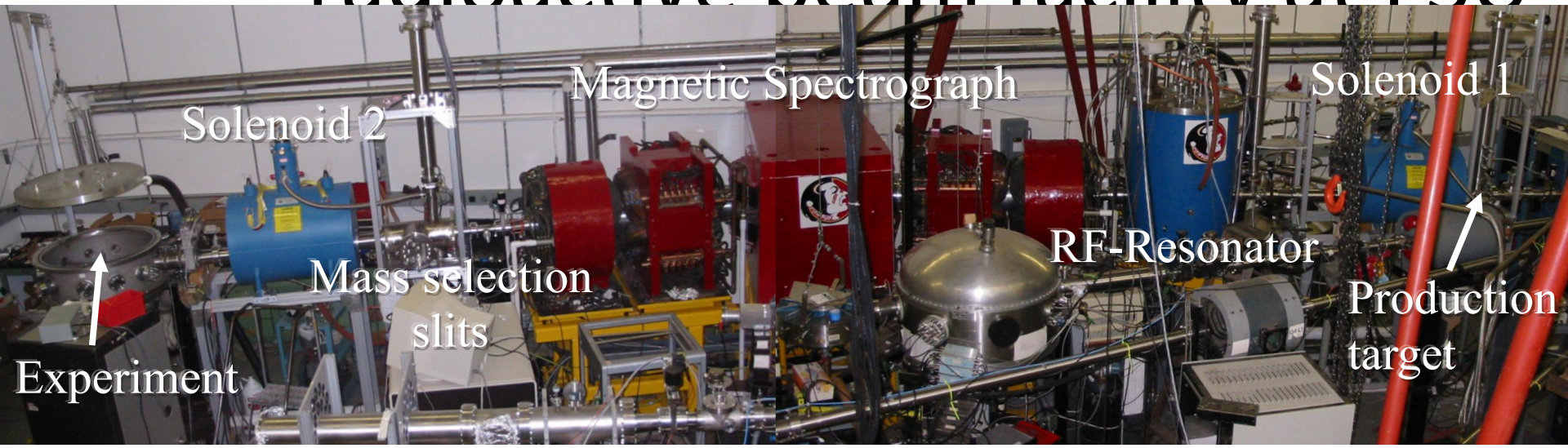

- In-flight production of radioactive beams in inverse kinematics
- Combination of Superconducting RF-Resonator with high acceptance magnetic Spectrograph to create mass spectrometer for E~5 MeV/u secondary beams

What is this K business with cyclotron and magnetic spectrometers?

$$E(\text{MeV/amu}) = K(q/A)^2$$

where q is the charge of the accelerated ion and A its mass

Here K is 120-160

Caution- knowledge of nuclear structure and description of reactions that are used to extract the structure information are not independent

Caution-We work in the world of strong interactions and many body systems

Today I will talk about the spin forces in nuclear structure and reactions

In 1932 deuterium or ^{2}H was isolated and this then explained why the masses of the elements are not integers.
For example: the atomic mass of Li is 6.941 with 92.4% ^{7}Li and 7.6% ^{6}Li

It was noticed immediately that there were 10 stable Sn isotopes with proton number 50 and neutron numbers from 62 to 74. Also was soon discovered that ^{208}Pb with 82 protons and 126 neutrons was very stable, as no decay was found from it.

There are elements that are chemically very stable with electron numbers
2.He,10,Ne,18,Ar,36,Kr,54,Xe,86,Rn
These are known as noble gases

Nuclear shell structure would be $(s_{1/2})2$, $(p_{3/2},p_{1/2})8$
$(d_{5/2},d_{3/2},s_{1/2})20$, $(f_{7/2},f_{5/2}.p_{3/2}.p_{1/2})40$
$(g_{9/2},g_{7/2},d_{5/2},d_{3/2},s_{1/2})70$
$(h_{11/2},h_{9/2},f_{7/2},f_{5/2},p_{3/2},p_{1/2})112$
$(i_{13/2},i_{11/2},g_{9/2}$ etc)168

It was known that the fine structure in atoms comes from the spin-orbit interaction but because the mass of the electron is in the denominator, a similar nuclear force
would be 2000 times weaker and so not important

Based on number of stable isotopes It was proposed that nuclei with proton or neutron numbers of 2,8,20,28,50,82,126 would be very stable and were called magic numbers

occur because nuclei have a large spin-orbit force of opposite sign from atoms

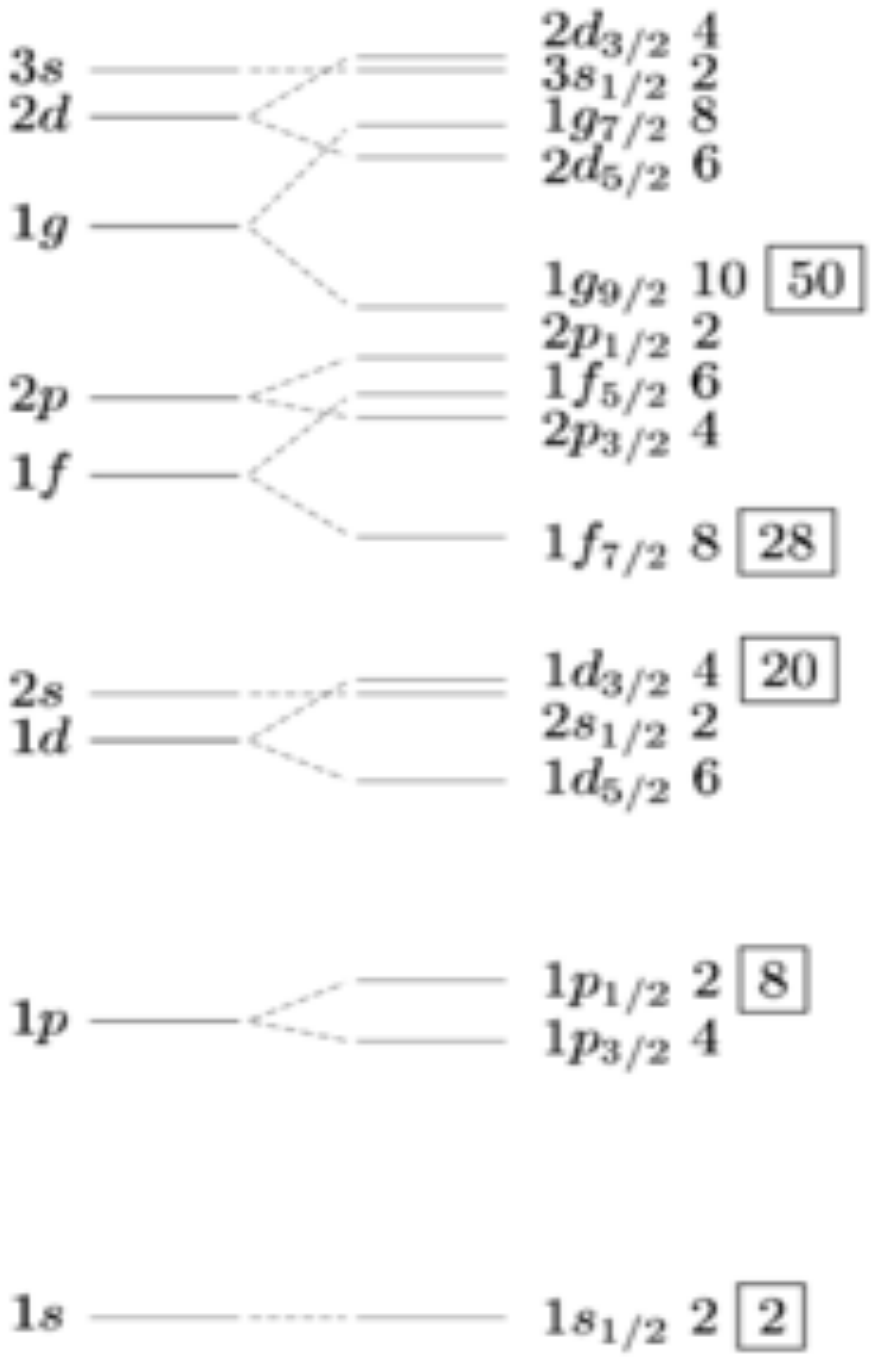
3s
2d
1g
2p
1f
2s
1d
1p
1s
2d3/2 4
3s1/2 2
1g7/2 8
2d5/2 6
1g9/2 10 50
2p1/2 2
1f5/2 6
2p3/2 4
1f7/2 8 28
1d3/2 4 20
2s1/2 2
1d5/2 6
1p1/2 2 8
1p3/2 4
1s1/2 2 2

New phenomena near n drip line: Modification of shell structure

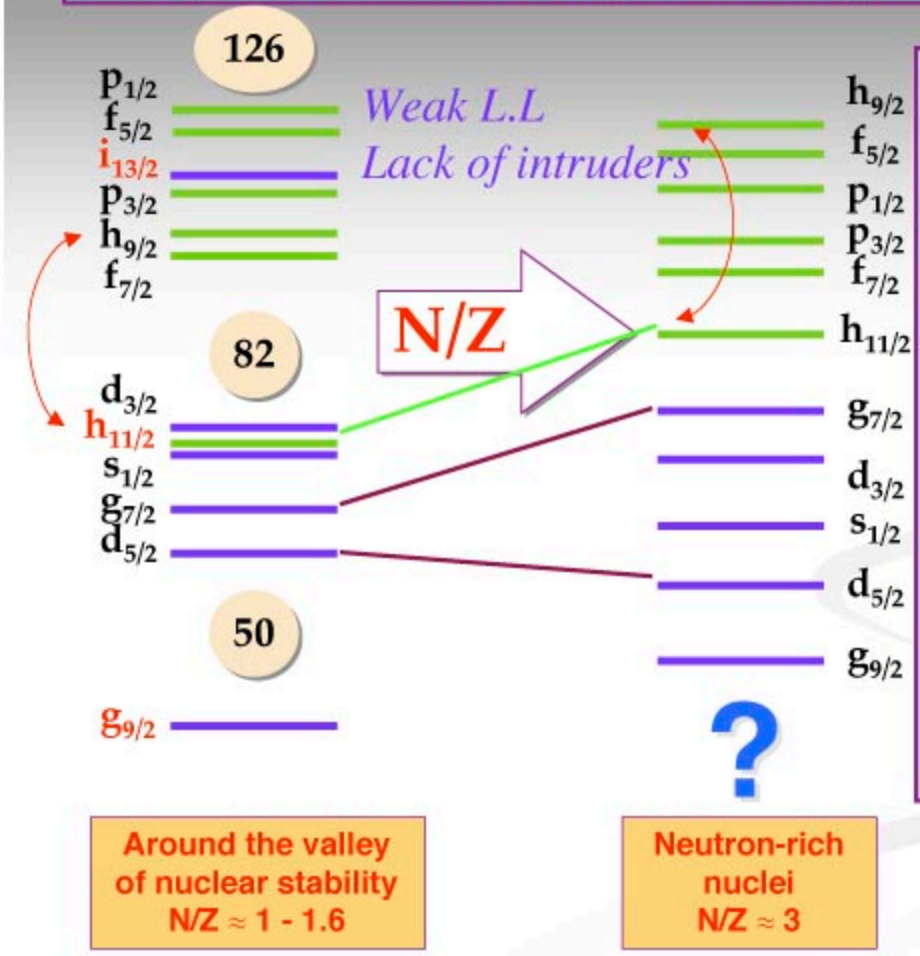

Around the valley of nuclear stability
N/Z ≈ 1 - 1.6

Neutron-rich nuclei
N/Z ≈ 3

Questions:

- **What is the shell structure near neutron drip line?**
- ***How to experimentally recognize the new features or new magic numbers?***
- ***Isotopic & isotonic trends also reflect p-n interactions!***

PR 75 (1949) 1766 cited 153

Total Reflection of Neutrons on Cobalt

MORTON HAMERMESH
Argonne National Laboratory, Chicago, Illinois
April 13, 1949

ATTENTION has recently been called to the possibility of producing polarized neutron beams by reflection from magnetized iron mirrors.[1] The indices of refraction differ for the two neutron spin states, since their magnetic scattering amplitudes are opposite in sign. The resultant difference in critical angle of total reflection can be used to separate the spin components.

For Fe, the coherent nuclear amplitude exceeds the magnetic amplitude, so that the index of refraction is less than one for both spin states, and both are capable of total reflection. Since the critical angle is proportional to neutron wavelength, two wave-lengths (one for each spin state) will overlap. This circumstance prevents attainment of complete polarization, since intensity requirements dictate the use of a fairly broad band of neutron energies.

It is interesting to note that by reflecting neutrons from a cobalt mirror magnetized along the beam direction one can obtain an exact analog of the Nicol prism. The coherent scattering cross section of Co is $\sim$1.8 barns[2] compared to 10.3 barns for Fe. At the same time, the magnetic amplitude for Co is $\sim 4.6\times10^{-13}$ cm, which is only slightly below the value 6.0×10^{-13} for Fe, so that for Co the magnetic amplitude *exceeds* the nuclear amplitude. Consequently, the refractive indices for the two spin states lie on opposite sides of unity for *all* wave-lengths, and only one of the spin components is capable of undergoing total reflection. With an arbitrarily broad spectrum of incident neutrons, the mirror will reflect a completely polarized beam.

D. J. Hughes and his associates are now conducting reflection experiments with Fe and Co.

[1] O. Halpern, Phys. Rev. **75**, 343 (1949).
[2] C. G. Shull and E. O. Wollan, unpublished.

On the "Magic Numbers" in Nuclear Structure

OTTO HAXEL
Max Planck Institut, Göttingen
J. HANS D. JENSEN
Institut f. theor. Physik, Heidelberg
AND
HANS E. SUESS
Inst. f. phys. Chemie, Hamburg
April 18, 1949

A SIMPLE explanation of the "magic numbers" 14, 28, 50, 82, 126 follows at once from the oscillator model of the nucleus,[1] if one assumes that the spin-orbit coupling in the Yukawa field theory of nuclear forces leads to a strong splitting of a term with angular momentum l into two distinct terms $j=l\pm\frac{1}{2}$.

If, as a first approximation, one describes the field potential of the nucleons already present, acting on the last one added, as that due to an isotropic oscillator, then the energy levels are characterized by a single quantum number $r=r_1+r_2+r_3$, where r_1, r_2, r_3 are the quantum numbers of the oscillator in 3 orthogonal directions. Table I, column 2 shows the multiplicity of a term with a given value of r, column 3 the sum of all multiplicities up to and including r. Isotropic anharmonicity of the potential field leads to a splitting of each r-term according to the orbital angular momenta l (l even when r is odd, and vice versa), as in Table I, column 4. Finally, spin-orbit coupling leads to the l-term splitting into $j=l\pm\frac{1}{2}$, columns 5 and 6, whose multiplicities are listed in column 7.

The "magic numbers" (column 8) follow at once on the assumption of a particularly marked splitting of the term with the highest angular momentum, resulting in a "closed shell structure" for each completed r-group, together with the highest j-term of the next succeeding r-group. This classification of states is in good agreement with the spins and magnetic moments of the nuclei with odd mass number, so far as they are known at present. The anharmonic oscillator model seems to us preferable to the potential well model,[2] since the range of the nuclear forces is not notably smaller than the nuclear radius.

A more detailed account will appear in three communications to Naturwissenschaften.[3]

TABLE I. Classification of nuclear states.

1 Oscillator-quantum number r	2 Multiplicity	3 Sum of all multiplicities	4 Orbital momentum l	5 Total angular momentum j	6 l_j-symbol	7 Multiplicities	8 Magic numbers
1	2	2	0	1/2	$s_{1/2}$	2	
2			1	3/2	$p_{3/2}$	4	
	6	8		1/2	$p_{1/2}$	2	
3			2	5/2	$d_{5/2}$	6	14
				3/2	$d_{3/2}$	4	
	12	20	0	1/2	$s_{1/2}$	2	
4			3	7/2	$f_{7/2}$	8	28
				5/2	$f_{5/2}$	6	
			1	3/2	$p_{3/2}$	4	
	20	40		1/2	$p_{1/2}$	2	
5			4	9/2	$g_{9/2}$	10	50
				7/2	$g_{7/2}$	8	
			2	5/2	$d_{5/2}$	6	
				3/2	$d_{3/2}$	4	
	30	70	0	1/2	$s_{1/2}$	2	
6			5	11/2	$h_{11/2}$	12	82
				9/2	$h_{9/2}$	10	
			3	7/2	$f_{7/2}$	8	
				5/2	$f_{5/2}$	6	
			1	3/2	$p_{3/2}$	4	
	42	112		1/2	$p_{1/2}$	2	
7			6	13/2	$i_{13/2}$	14	126
				11/2	$i_{11/2}$	12	
			4	9/2	$g_{9/2}$	10	

[1] See, e.g., H. A. Bethe and R. Bacher, Rev. Mod. Phys. **8**, 82 (1937), pars. 32–34.
[2] Which anyhow does not lead to a very different term-sequence compared with that of an anharmonic oscillator, see reference 1.
[3] (a) Haxel, Jensen, and Suess, Naturwiss. (in press). (b) Suess, Haxel, and Jensen, Naturwiss. (in press). (c) Jensen, Suess, and Haxel, Naturwiss. (in press).

Concerning the Abundance of Atmospheric Carbon Monoxide

ARTHUR ADEL
Arizona State College, Flagstaff, Arizona
April 19, 1949

IN October of 1941 the 4.7-micron region of the solar spectrum was examined by the author at the Lowell Observatory, Flagstaff, for evidence of the carbon monoxide fundamental. The observation was made with a 2400-lines/inch grating in an $f/5$-Pfund type spectrometer of focal length 30 inches. Galvanometer deflections were recorded photographically. The solar spectrum was compared with laboratory observations,[1] but no conclusive evidence could be deduced for the existence of spectroscopically detectable quantities of carbon monoxide in the atmosphere above the observatory. The adequacy of the solar spectrum can be judged from the fact that carbon dioxide fine structure (some of it since traced to ν_3 of $C^{13}O_2^{16}$), which is twice as difficult to resolve as carbon monoxide fine structure, was abundantly present and clearly resolved.

One notes with interest, therefore, Migeotte's recent observation of the carbon monoxide fundamental as a prominent feature in the solar spectrum at Columbus, Ohio.[2]

The purely local nature of atmospheric abundance of carbon monoxide is emphasized by its absence over Flagstaff,

Cited 139

THE
PHYSICAL REVIEW

A journal of experimental and theoretical physics established by E. L. Nichols in 1893

SECOND SERIES, VOL. 74, NO. 3 AUGUST 1, 1948

On Closed Shells in Nuclei*

MARIA G. MAYER
Argonne National Laboratory and Institute for Nuclear Studies, University of Chicago, Chicago, Illinois
(Received April 16, 1948)

Experimental facts are summarized to show that nuclei with 20, 50, 82, or 126 neutrons or protons are particularly stable.

IT has been suggested in the past that special numbers of neutrons or protons in the nucleus form a particularly stable configuration.[1] The complete evidence for this has never been summarized, nor is it generally recognized how convincing this evidence is. That twenty neutrons or protons (Ca^{40}) form a closed shell is predicted by the Hartree model. A number of calculations support this fact.[2] These considerations will not be repeated here. In this paper, the experimental facts indicating a particular stability of shells of 50 and 82 protons and of 50, 82, and 126 neutrons will be listed.

I. ISOTOPIC ABUNDANCES

The discussion in this section will be mostly confined to the heavy elements, which for this purpose may be defined as those with atomic number greater than 33; selenium would be the first "heavy" element. For these elements, the isotopic abundances show a number of striking regularities which are violated in very few cases.

(a) For elements with even Z, the relative abundance of a single isotope is not greater than 60 percent. This becomes more pronounced with increasing Z; for $Z>40$, relative abundances greater than 35 percent are not encountered. The exceptions to this rule are given in Table I.

(b) The isotopic abundances are not symmetrically distributed around the center, but the light, neutron-poor isotopes have low abundances. The concentration of the lightest isotope is, as a rule, less than 2 percent. The exceptions to this rule are listed in Table II.

It is seen that the violations of these two regularities occur practically only at neutron numbers 50 and 82. Only the case of ruthenium in Table II, which is not a very pronounced exception, does not fall into one of these groups.

The case of samarium, where the lightest isotope has an isotopic abundance of 3 percent, is only a bare violation of the rule and may not seem striking. However, what is extraordinary, the next heavier even isotope of samarium, Sm^{146} with 84 neutrons, which one would expect to find in greater concentration, does not exist at all.

II. NUMBER OF ISOTONES

Figures 1 and 2 reproduce the parts of the table by Segrè in the region of nuclei with 50

* This document is based on work performed under Contract Number W-31-109-eng-38 for the Atomic Energy Commission at the Argonne National Laboratory. Submitted for declassification on February 13th, 1948.
[1] W. Elsasser, J. de phys. et rad. **5**, 625 (1934).
[2] E. Wigner, Phys. Rev. **51**, 947 (1937); W. H. Barkas, Phys. Rev. **55**, 691 (1939).

PR 76 (1949) Page 1969

since a rigid or liquid nucleus as a whole would have no orbital momentum in its lowest state.

The scheme proposed by Mayer follows exactly the order in a potential well. It achieves the breaks at the correct places by the assumption of a very strong spin-orbit coupling at high angular momentum values.

A summary of the three schemes is given in Table I. All three schemes give, of course, the empirical shell numbers and a statistical correlation with observed spins and moments. A decision between the schemes may be hoped for through discussion of new data which may tend to tip the scales in a definite direction, or by more theoretical work. Among the latter would be a refined calculation of the effects of the Coulomb forces on the density distribution in a nucleus, improved treatment of the many body problem, and better understanding of the spin-orbit coupling in nuclei.

It should be emphasized that the existence and the characteristics of nuclear shell structure have become now much more clearly established than formerly in spite of the ambiguities in their interpretation. Particularly there is a definite correlation between spin and shell structure. This does not mean necessarily that the individual particle model is better than hitherto assumed. The shell structure in nuclei, is, however, so pronounced an effect that one may hope to obtain an interpretation even on basis of such a crude approximation as the individual particle model.

* This letter has been written on request by the editor of the Physica Review, who received the papers, reference 1 and 2, by the same mail.
[1] Eugene Feenberg and Kenyon C. Hammack, Phys. Rev. **75**, 1877 (1949).
[2] L. W. Nordheim, Phys. Rev. **75**, 1894 (1949).
[3] Maria G. Mayer, Phys. Rev. **75**, 1969 (1949).

On Closed Shells in Nuclei. II

MARIA GOEPPERT MAYER
Argonne National Laboratory and Department of Physics, University of Chicago, Chicago, Illinois

February 4, 1949

THE spins and magnetic moments of the even-odd nuclei have been used by Feenberg[1,2] and Nordheim[3] to determine the angular momentum of the eigenfunction of the odd particle. The tabulations given by them indicate that spin orbit coupling favors the state of higher total angular momentum. If strong spin-orbit coupling, increasing with angular momentum, is assumed, a level assignment different from either Feenberg or Nordheim is obtained. This assignment encounters a very few contradictions with experimental facts and requires no major crossing of the levels from those of a square well potential. The magic numbers 50, 82, and 126 occur at the place of the spin-orbit splitting of levels of high angular momentum.

Table I contains in column two, in order of decreasing binding energy, the levels of the square well potential. The quantum number gives the number of radial nodes. Two levels of the same quantum number cannot cross for any type of potential well, except due to spin-orbit splitting. No evidence of any crossing is found. Column three contains the usual spectroscopic designation of the levels, as used by Nordheim and Feenberg. Column one groups together those levels which are degenerate for a three-dimensional isotropic oscillator potential. A well with rounded corners will have a behavior in between these two potentials. The shell grouping is given in column five, with the numbers of particles per shell and the total number of particles up to and including each shell in column six and seven, respectively.

Within each shell the levels may be expected to be close in energy, and not necessarily in the order of the table, although the order of levels of the same orbital angular momentum and different spin should be maintained. Two exceptions, $_{11}Na^{23}$ with spin 3/2 in stead of the expected $d_{5/2}$, and$_{25}$ Mn^{55} with 5/2 instead of the expected $f_{7/2}$, are the only violations.

Table II lists the known spins and orbital assignments from magnetic moments[4] when these are known and unambiguous, for the even-odd nuclei up to 83. Beyond 83 the data is limited and no exceptions to the assignment appear.

Up to Z or $N=20$, the assignment is the same as that of Feenberg and Nordheim. At the beginning of the next shell, $f_{7/2}$ levels occur at 21 and 23, as they should. At 28 the $f_{7/2}$ levels should be filled, and no spins of 7/2 are encountered any more in this shell. This subshell may contribute to the stability of Ca^{48}. If the $g_{9/2}$ level did not cross the $p_{1/2}$ or $f_{5/2}$

TABLE I.

Osc. No.	Square well	Spect. term	Spin term	No. of states	Shells	Total No.
0	$1s$	$1s$	$1s_{1/2}$	2	2	2
			$1p_{1/2}$	4		
1	$1p$	$2p$	$1p_{3/2}$	2	6	8
	$1d$	$3d$	$1d_{5/2}$	6		
2			$1d_{3/2}$	4	12	
	$2s$	$2s$	$2s_{1/2}$	2		20
			$1f_{7/2}$	8	8?	28?
	$1f$	$4f$	$1f_{5/2}$	6		
3			$2p_{3/2}$	4	22	
	$2p$	$3p$	$2p_{1/2}$	2		
			$1g_{9/2}$	10		50
	$1g$	$5g$				
			$1g_{7/2}$	8		
4	$2d$	$4d$	$2d_{5/2}$	6		
			$2d_{3/2}$	4	32	
	$3s$	$3s$	$3s_{1/2}$	2		
			$1h_{11/2}$	12		82
	$1h$	$6h$				
			$1h_{9/2}$	10		
			$2f_{7/2}$	8		
5	2	$5f$	$2f_{5/2}$	6		
			$3p_{3/2}$	4	44	
	$3p$	$4p$	$3p_{1/2}$	2		
			$1i_{13/2}$	14		126
	$1i$	$7i$				
			$1i_{11/2}$			
6	$2g$	$6g$				
	$3d$	$5d$				
	$4s$	$4s$				

levels, the first spin of 9/2 should occur at 41, which is indeed the case. Three nuclei with N or $Z=49$ have $g_{9/2}$ orbits. No s or d levels should occur in this shell and there is no evidence for any.

The only exception to the proposed assignment in this shell is the spin 5/2 instead of 7/2 for Mn^{55}, and the fact that the magnetic moment of $_{27}Co^{59}$ indicates a $g_{7/2}$ orbit instead of the expected $f_{7/2}$.

In the next shell two exceptions to the assignment occur. The spin of 1/2 for Mo^{95} with 53 would be a violation, but is experimentally doubtful. The magnetic moment of Eu^{153} indicates $f_{5/2}$ instead of the predicted $d_{5/2}$. No $h_{11/2}$ levels appear. It seems that these levels are filled in pairs only,

Thanks are due to Enrico Fermi for the remark "Is there any indication of spin-orbit coupling?" which was the origin of this paper.

Signatures of large shell gaps & magic numbers

Combinations of:

- **Kinks in *1n* and *2n* separation energies**
- **Large E(2⁺) and small B(E2) -- signature of rigid spheres**
- **Small σ(n,γ) (peaks in element abundances)**
- **Kinks in single-particle energies**
- **Kinks in radii**

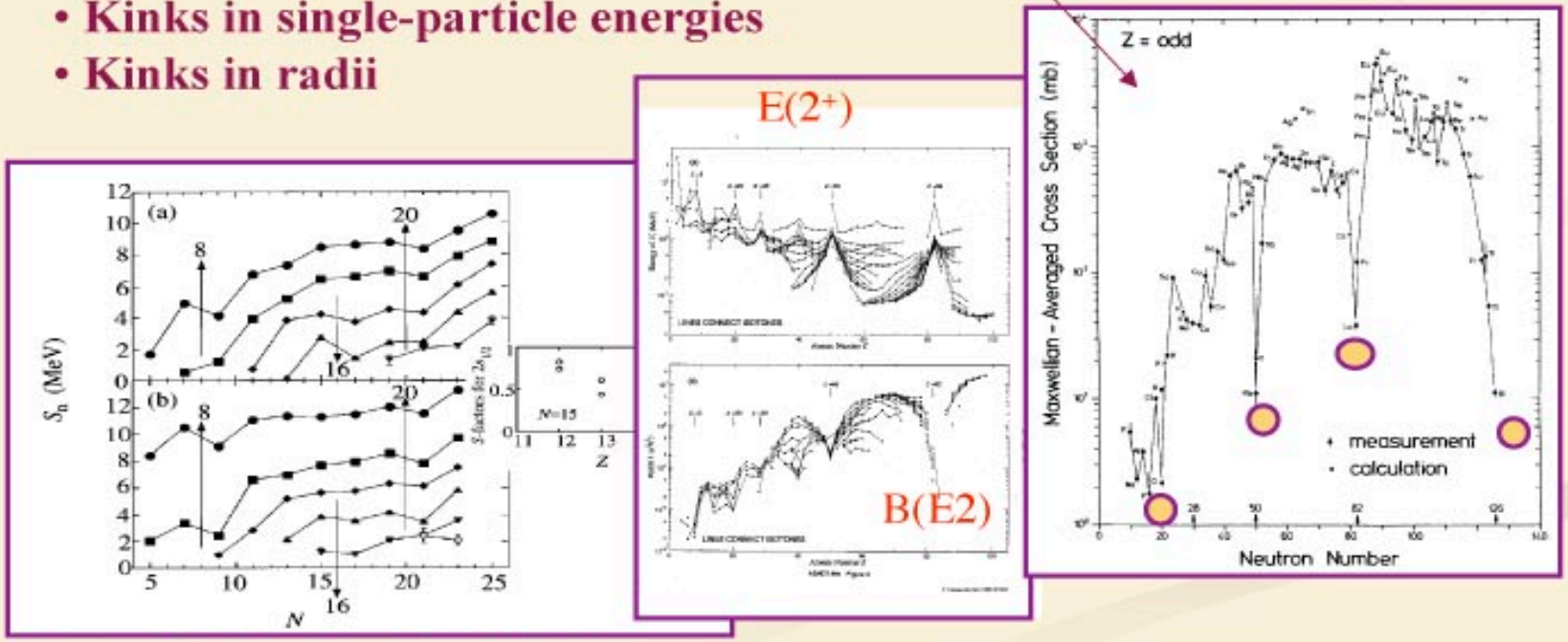

Ozawa *et al.*, Phys. Rev. Lett. 84 (2000) 5493

We can use current machines to test shell model calculations as they predict where the neutron drip line will occur

Predict ^{28}O stable

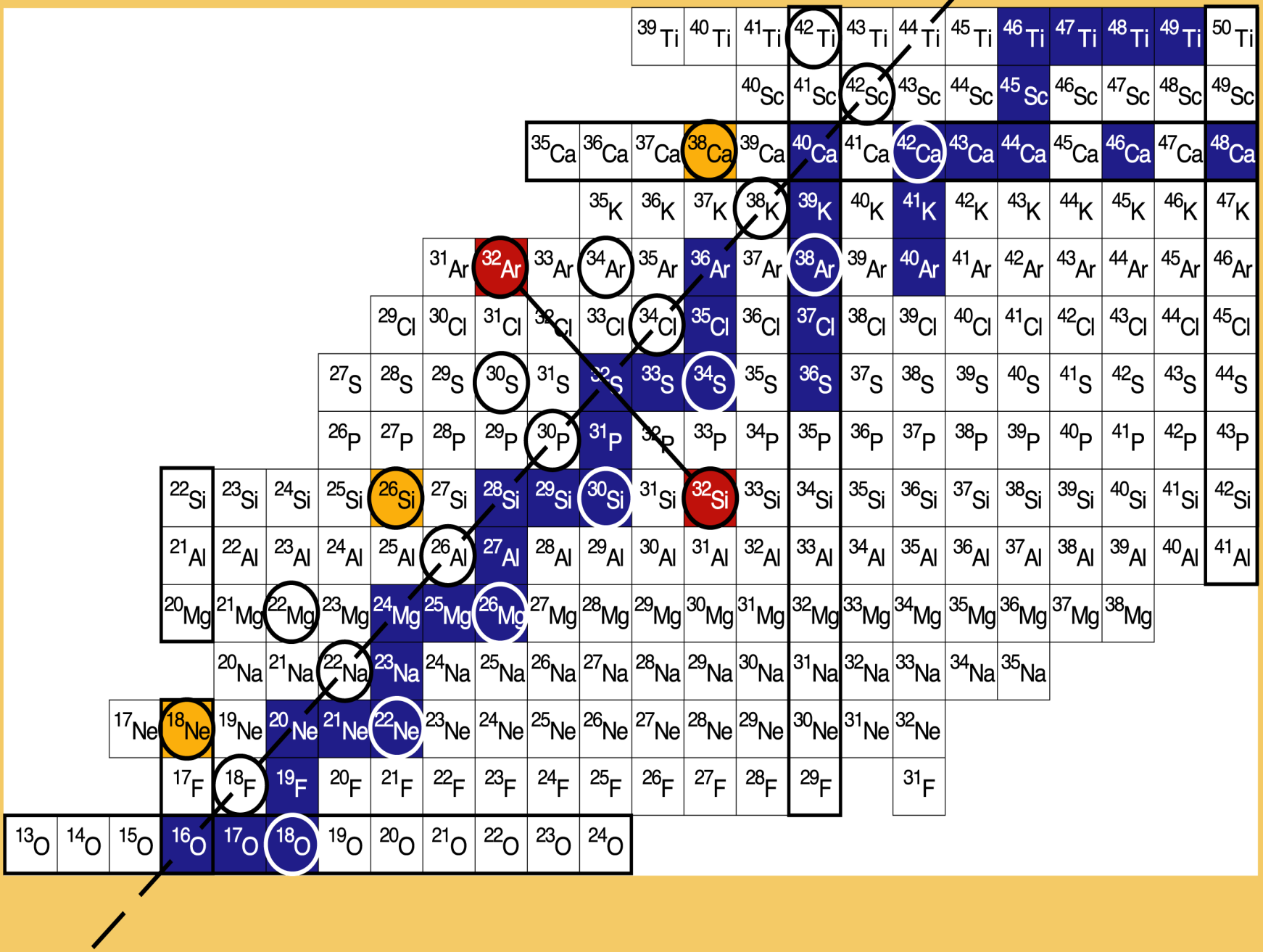
39Ti 40Ti 41Ti 42Ti 43Ti 44Ti 45Ti 46Ti 47Ti 48Ti 49Ti 50Ti
40Sc 41Sc 42Sc 43Sc 44Sc 45Sc 46Sc 47Sc 48Sc 49Sc
35Ca 36Ca 37Ca 38Ca 39Ca 40Ca 41Ca 42Ca 43Ca 44Ca 45Ca 46Ca 47Ca 48Ca
35K 36K 37K 38K 39K 40K 41K 42K 43K 44K 45K 46K 47K
31Ar 32Ar 33Ar 34Ar 35Ar 36Ar 37Ar 38Ar 39Ar 40Ar 41Ar 42Ar 43Ar 44Ar 45Ar 46Ar
29Cl 30Cl 31Cl 32Cl 33Cl 34Cl 35Cl 36Cl 37Cl 38Cl 39Cl 40Cl 41Cl 42Cl 43Cl 44Cl 45Cl
27S 28S 29S 30S 31S 32S 33S 34S 35S 36S 37S 38S 39S 40S 41S 42S 43S 44S
26P 27P 28P 29P 30P 31P 32P 33P 34P 35P 36P 37P 38P 39P 40P 41P 42P 43P
22Si 23Si 24Si 25Si 26Si 27Si 28Si 29Si 30Si 31Si 32Si 33Si 34Si 35Si 36Si 37Si 38Si 39Si 40Si 41Si 42Si
21Al 22Al 23Al 24Al 25Al 26Al 27Al 28Al 29Al 30Al 31Al 32Al 33Al 34Al 35Al 36Al 37Al 38Al 39Al 40Al 41Al
20Mg 21Mg 22Mg 23Mg 24Mg 25Mg 26Mg 27Mg 28Mg 29Mg 30Mg 31Mg 32Mg 33Mg 34Mg 35Mg 36Mg 37Mg 38Mg
20Na 21Na 22Na 23Na 24Na 25Na 26Na 27Na 28Na 29Na 30Na 31Na 32Na 33Na 34Na 35Na
17Ne 18Ne 19Ne 20Ne 21Ne 22Ne 23Ne 24Ne 25Ne 26Ne 27Ne 28Ne 29Ne 30Ne 31Ne 32Ne
17F 18F 19F 20F 21F 22F 23F 24F 25F 26F 27F 28F 29F 31F
13O 14O 15O 16O 17O 18O 19O 20O 21O 22O 23O 24O

New phenomena near n drip line: Modification of shell structure

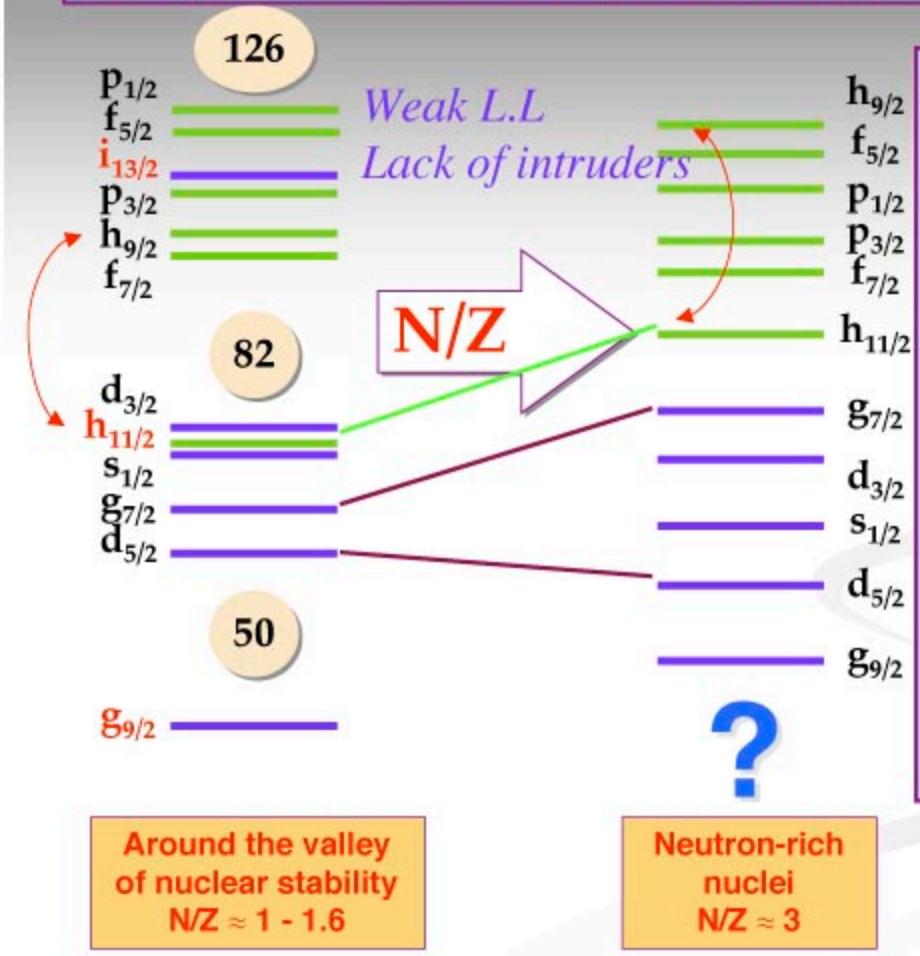

Around the valley of nuclear stability
N/Z ≈ 1 - 1.6

Neutron-rich nuclei
N/Z ≈ 3

Questions:

- **What is the shell structure near neutron drip line?**
- ***How to experimentally recognize the new features or new magic numbers?***
- ***Isotopic & isotonic trends also reflect p-n interactions!***

The "Island of Inversion" – A brief history

C. Thibault et al: ^{31,32}Na, local increase of S_{2n} → *N=20* shell closure would lead to a decrease
Phys. Rev. C 12, 646 (1975)

X. Campi et al: observation explained by deformation via filling of $\nu f_{7/2}$ in ^{31,32}Na
Nucl. Phys.. A 251, 193 (1975)

C. Detraz et al: ^{32}Na → ^{32}Mg β decay, low 2^+ in ^{32}Mg (885 keV)
Phys. Rev. C 19, 164 (1979)

B.H. Wildenthal et al: ^{31}Na,^{32}Mg isolated cases, less n-rich neighbors well understood in *sd* shell Phys. Rev. C 22, 2260 (1980)

E. Warburton, John A. Becker and B. A. Brown: *Z=10-12* and *N=20-22* have intruder ground state configurations $(sd)^{-2}(fp)^{+2}$
Phys. Rev. C 41, 1147 (1990)

neutron-*ph* excitations across the *N=20* shell gap

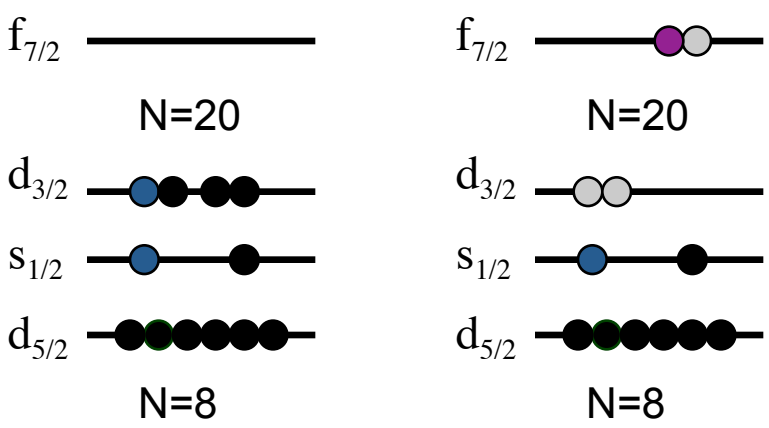

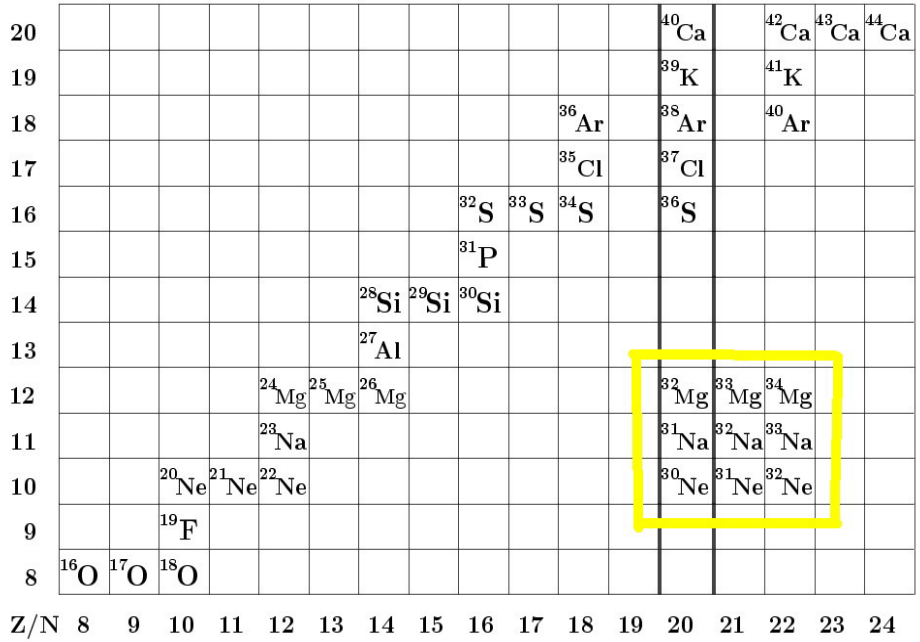

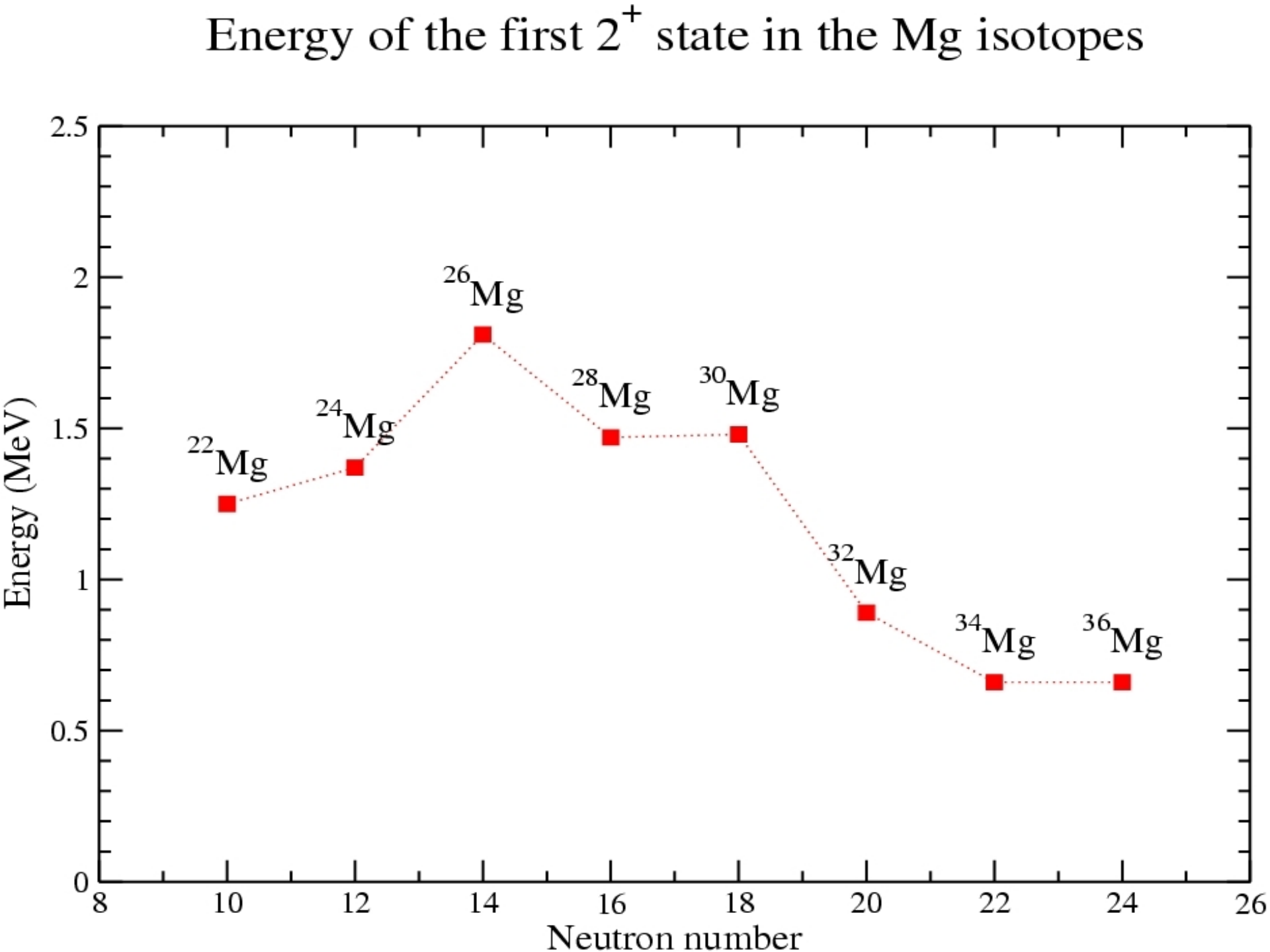
Energy of the first 2+ state in the Mg isotopes
Energy (MeV)
Neutron number
0
0.5
1
1.5
2
2.5
8
10
12
14
16
18
20
22
24
26
22Mg
24Mg
26Mg
28Mg
30Mg
32Mg
34Mg
36Mg

The Island of Inversion has been studied with beta decay (how the low lying 2+ was discovered) Coul Ex (fast beam at RIKEN and NSCL) slow beam at REX-ISOLODE, various stripping and pickup Reactions.

The main reason for this emphasis on the mass region around 32Mg is simply that it is the first experimentally accessible set of nuclei where the p-n interaction totally dominated the low lying structure

/hat

We also know ^{42}Si with 14 protons and 28 neutrons is deformed based on its first 2+ energy as is ^{44}S with 16 protons and 28 neutrons.

What about 46 Ar, with 18 protons and 28 neutrons? The last stable Ar isotope is 40. The first 2+ in 46 Ar is 1.58 MeV

Of course 48Ca with 20 protons and 28 neutrons looks spherical just to add to the confusion. Its first 2+ is at 3.8 MeV

Caution in jumping to conclusions about shell modification

"Single particle" orbitals are dressed even in magic nuclei

Importance of coupling of single-particles to 2^+ & 3^- phonons

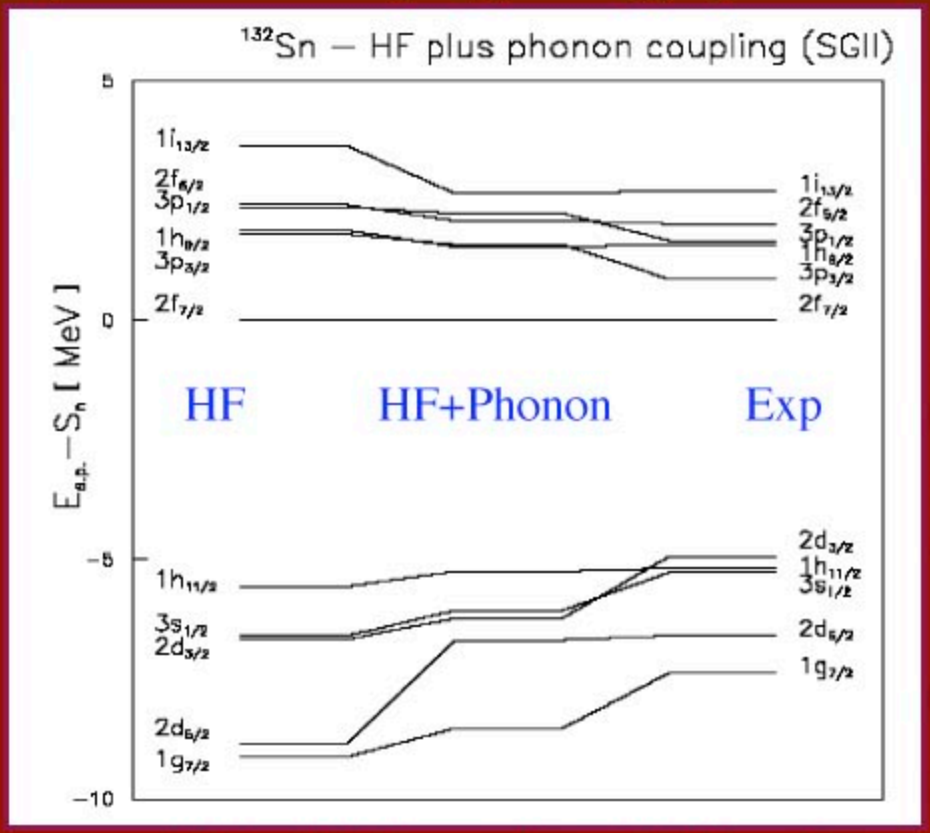

But note that the *p* orbitals are hardly affected!

p orbitals stay above experimental values.

Colo, Bortignon, Sarchi, Vigezzi

From many studies around the world at stable and radioactive beam laboratories, we now know that the magic numbers of 20 and 28 are not always magic.

In fact there are times when we see that neutron number 16 is magic.

The region around Z=12 and N=20 is now known as the island of inversion and arises because deformed and spherical shapes are very close together in energy. The structure studies have shown that knowledge of the p-n interaction is critical for any shell model to have a predictive power

As we began to think about what nuclear structure one would expect as you add neutrons since there was interest in building up the elements in stars through neutron capture, it was felt that something might happen to the magic numbers because the spin orbit should decrease since the neutrons are now only on the surface.

New phenomena near n drip line: Modification of shell structure

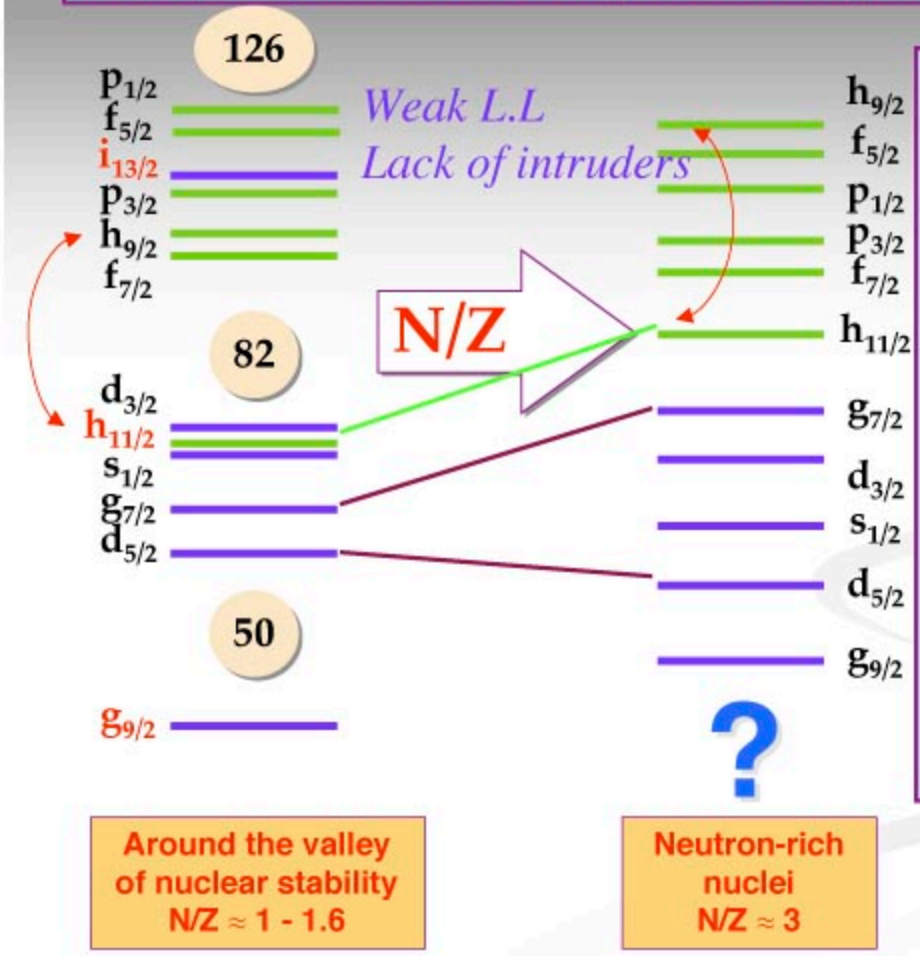

Around the valley of nuclear stability
N/Z ≈ 1 - 1.6

Neutron-rich nuclei
N/Z ≈ 3

Questions:

- **What is the shell structure near neutron drip line?**
- ***How to experimentally recognize the new features or new magic numbers?***
- ***Isotopic & isotonic trends also reflect p-n interactions!***

Remember, that the real puzzle was why Z or N =50 was magic and it is the spin orbit interaction that makes the g9/2 orbit drops down into the f-p shell causing the gap.

So to look for the decrease in spin orbit as a function of neutron number we will have to be able to study Ni 78, with 28 protons and 50 neutrons, a job for future labs.

Can we calculate the structure of light nuclei beginning from knowing two body interactions and then adding them up to produce the observed structure?

In early years (1985 or so) argument was made that with powerful computers could do so.
So now we can do these calculations, what happens?

Big Trouble

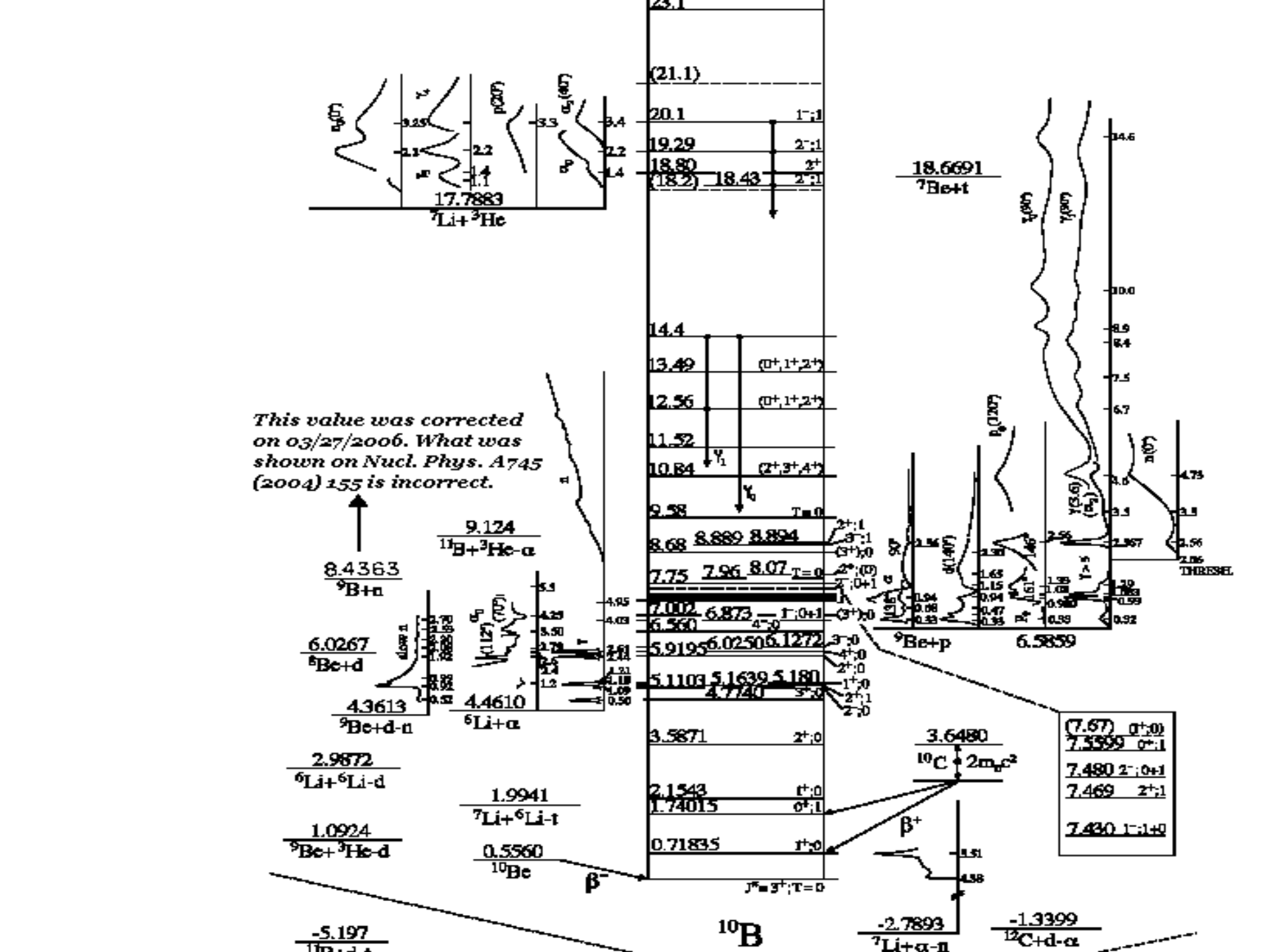
This value was corrected on 03/27/2006. What was shown on Nucl. Phys. A745 (2004) 155 is incorrect.
8.4363
^{9}B+n
9.124
^{11}B+^{3}He-α
6.0267
^{6}Be+d
4.3613
^{9}Be+d-n
4.4610
^{6}Li+α
2.9872
^{6}Li+^{6}Li-d
1.9941
^{7}Li+^{6}Li-t
1.0924
^{9}Be+^{3}He-d
0.5560
^{10}Be
β⁻
17.7883
^{7}Li+^{3}He
18.6691
^{7}Be+t
^{9}Be+p
6.5859
THRESH
3.6480
^{10}C
$2m_ec^2$
β⁺
-2.7893
^{7}Li+α-n
-1.3399
^{12}C+d-α
-5.197
^{10}B
J^π = 3^+; T = 0
(21.1)
20.1
19.29
18.80
(18.2)
18.43
14.4
13.49
12.56
11.52
10.84
9.58
8.68
8.889
8.894
7.75
7.96
8.07
7.002
6.873
6.560
5.9195
6.0250
6.1272
5.1103
5.1639
5.180
4.7740
3.5871
2.1543
1.74015
0.71835
(7.67)
7.5599
7.480
7.469
7.430

Next I want to consider a puzzle in some data just taken that involves polarization.

Some definitions for spin physics

$A(\vec{a},a)A$	Analyzing power
$A(a,\vec{a})A$	Polarization
$A(\vec{a},b)A$	Analyzing power
$A(a,\vec{b})A$	Polarization

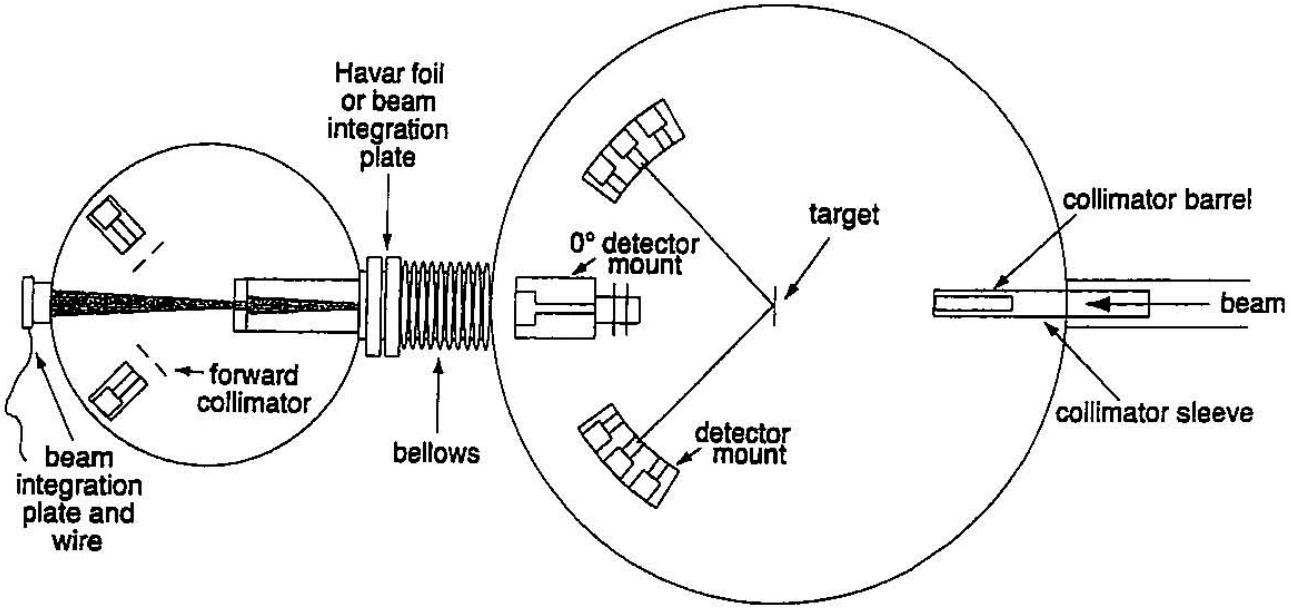

^{4}He POLARIMETER

85cm MAIN CHAMBER

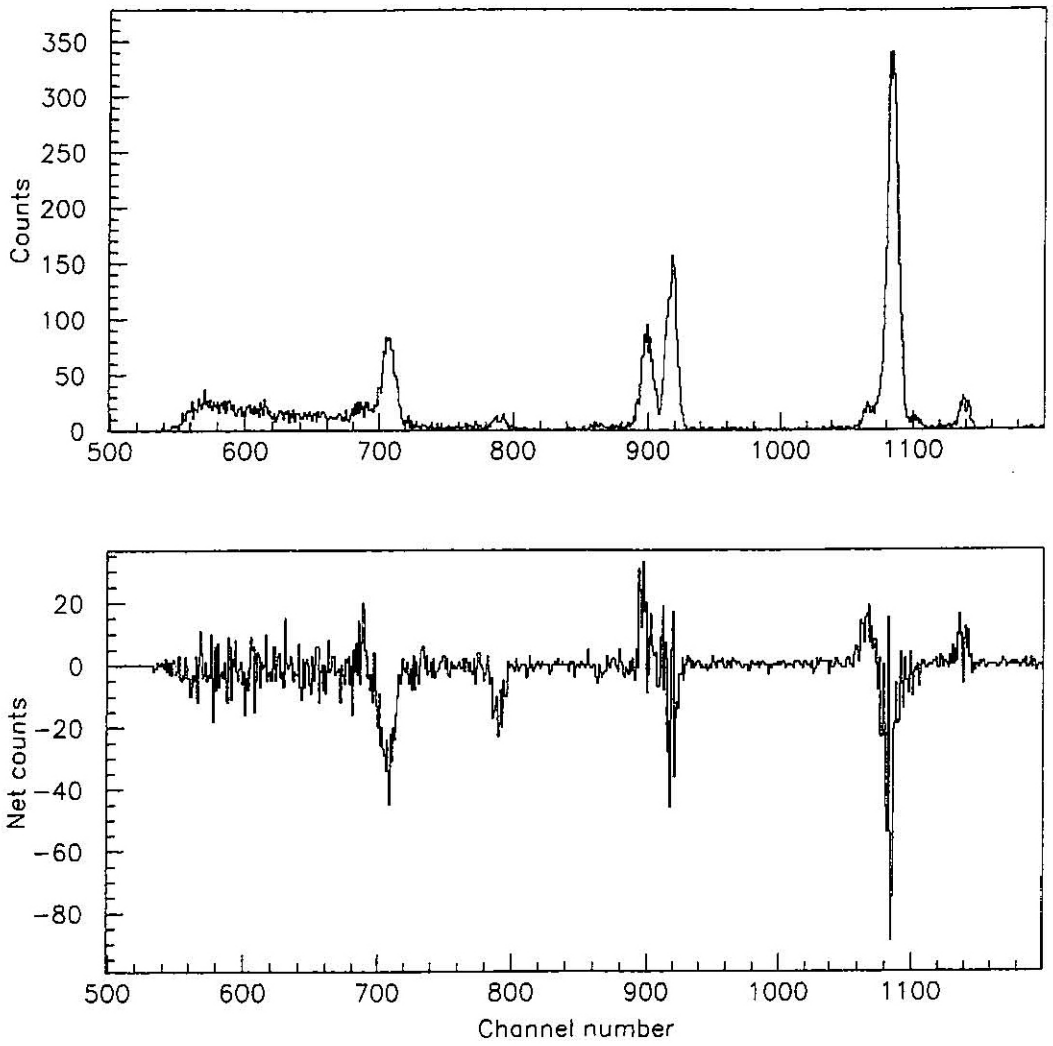

Spin up minus spin down to show there is an analyzing power for $^{7}\vec{\mathrm{Li}}+^{12}\mathrm{C}$

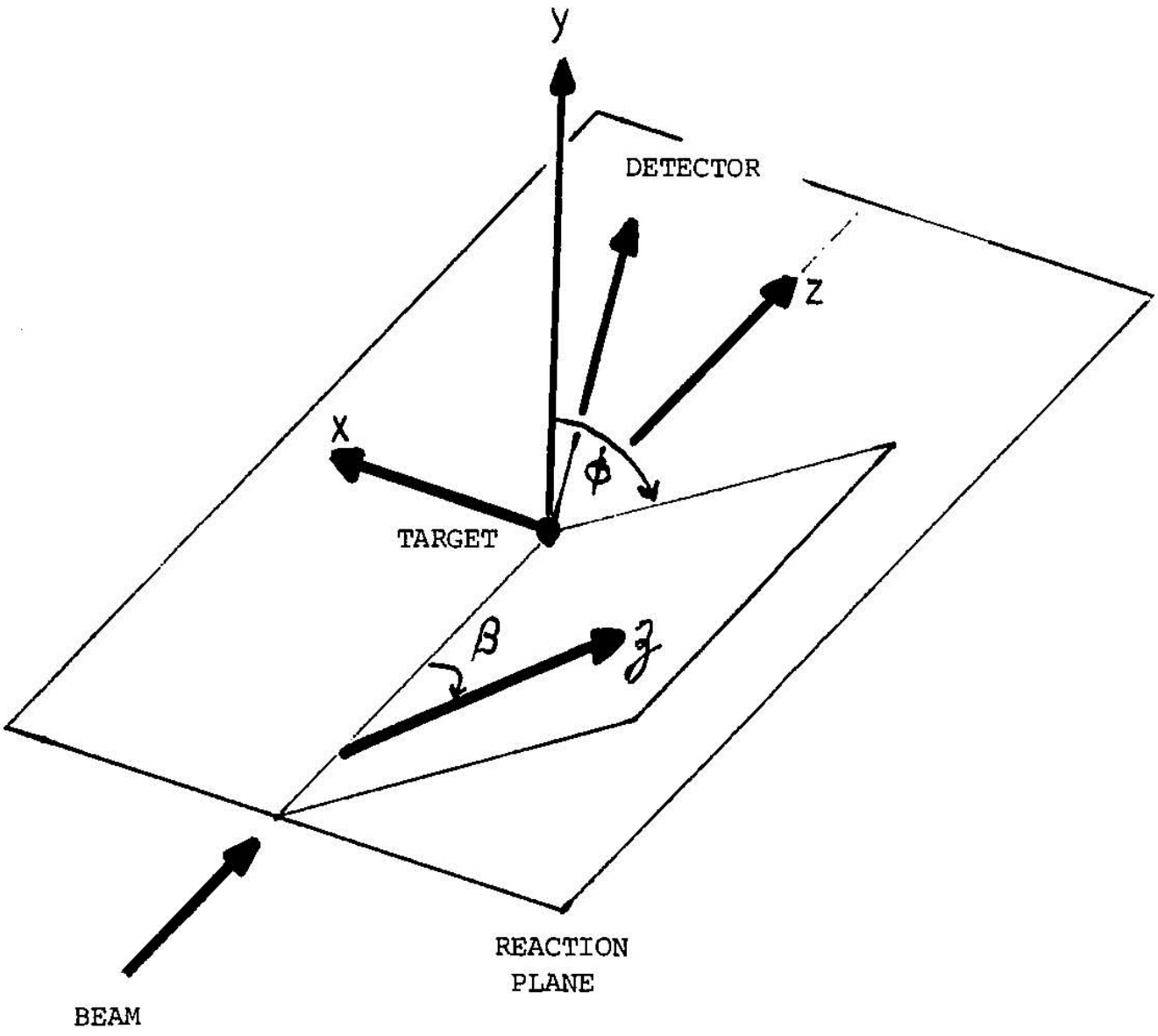
y
DETECTOR
z
x
φ
TARGET
β
z
REACTION
PLANE
BEAM

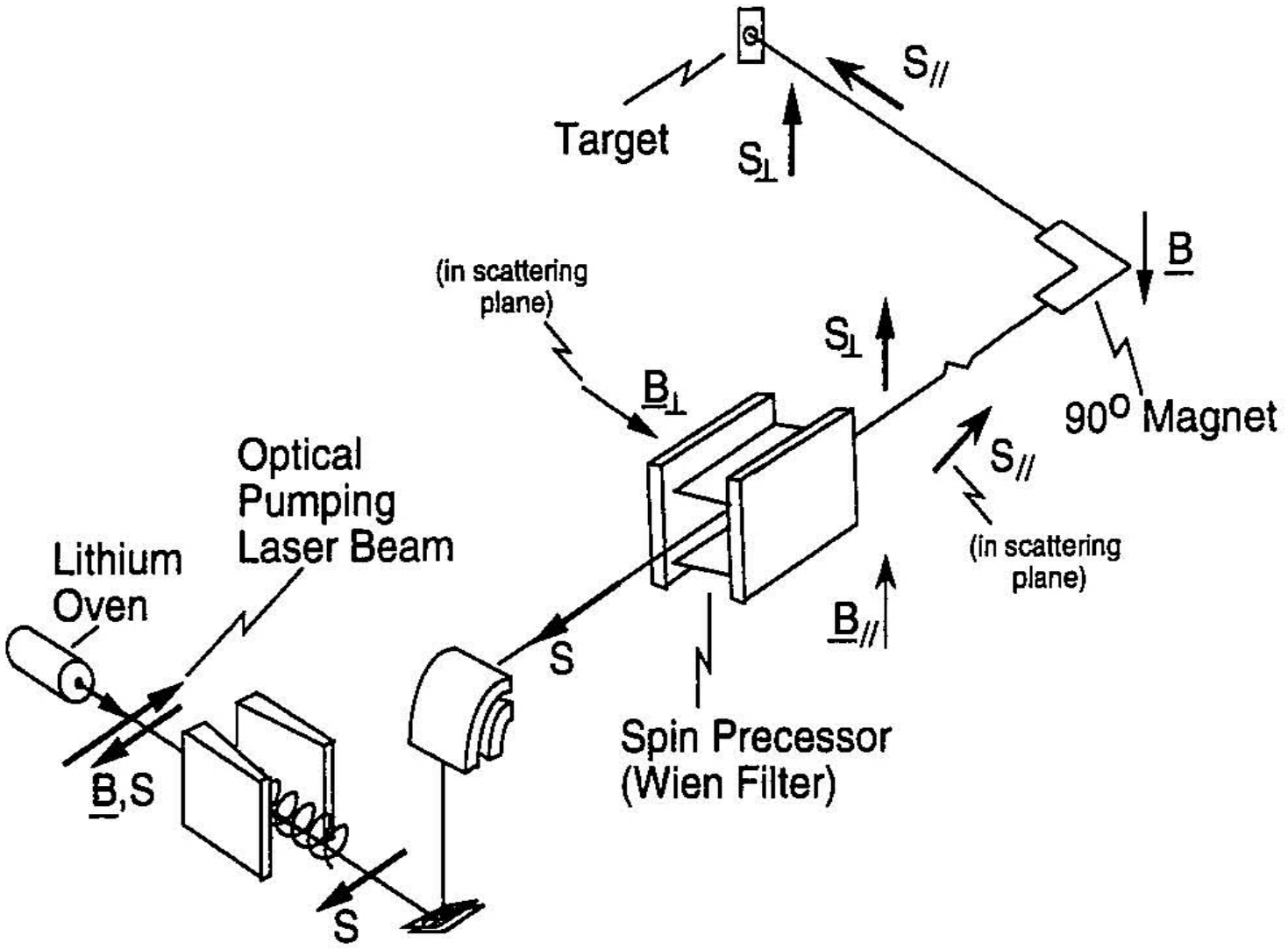
Target
$S_{//}$
$S_{\perp}$
B
(in scattering plane)
$B_{\perp}$
$S_{\perp}$
90° Magnet
$S_{//}$
(in scattering plane)
Optical Pumping Laser Beam
Lithium Oven
S
$B_{//}$
B,S
Spin Precessor (Wien Filter)
S

Using this rotation, the cross section σ_{pol} measured for a spin $\frac{3}{2}$ polarized beam is expanded in the Madison frame as

$$\sigma_{pol} = \sigma_{unp} \left[1 + \sqrt{2} \sin\beta \cos\phi \, t_{10} \, iT_{11} + \frac{1}{2}(3\cos^2\beta - 1) \, t_{20} \, T_{20} \right.$$

$$+ \sqrt{3/2} \sin 2\beta \sin\phi \, t_{20} \, T_{21} - \sqrt{3/2} \sin^2\beta \cos 2\phi \, t_{20} \, T_{22}$$

$$+ \frac{1}{2}\sqrt{3} \sin\beta \, (5\cos^2\beta - 1) \cos\phi \, t_{30} \, iT_{31}$$

$$\left. + \sqrt{15/8} \sin\beta \sin 2\beta \sin 2\phi \, t_{30} \, iT_{32} - \frac{1}{2}\sqrt{5} \sin^3\beta \cos 3\phi \, t_{30} \, iT_{33} \right],$$

$$R\text{-}L = 2\sqrt{2}(iT_{11} * t_{10})$$

$$Ay = (2/\sqrt{3})\ iT_{11} = (R\text{-}L)/\ (t_{10})\ \sqrt{6}$$

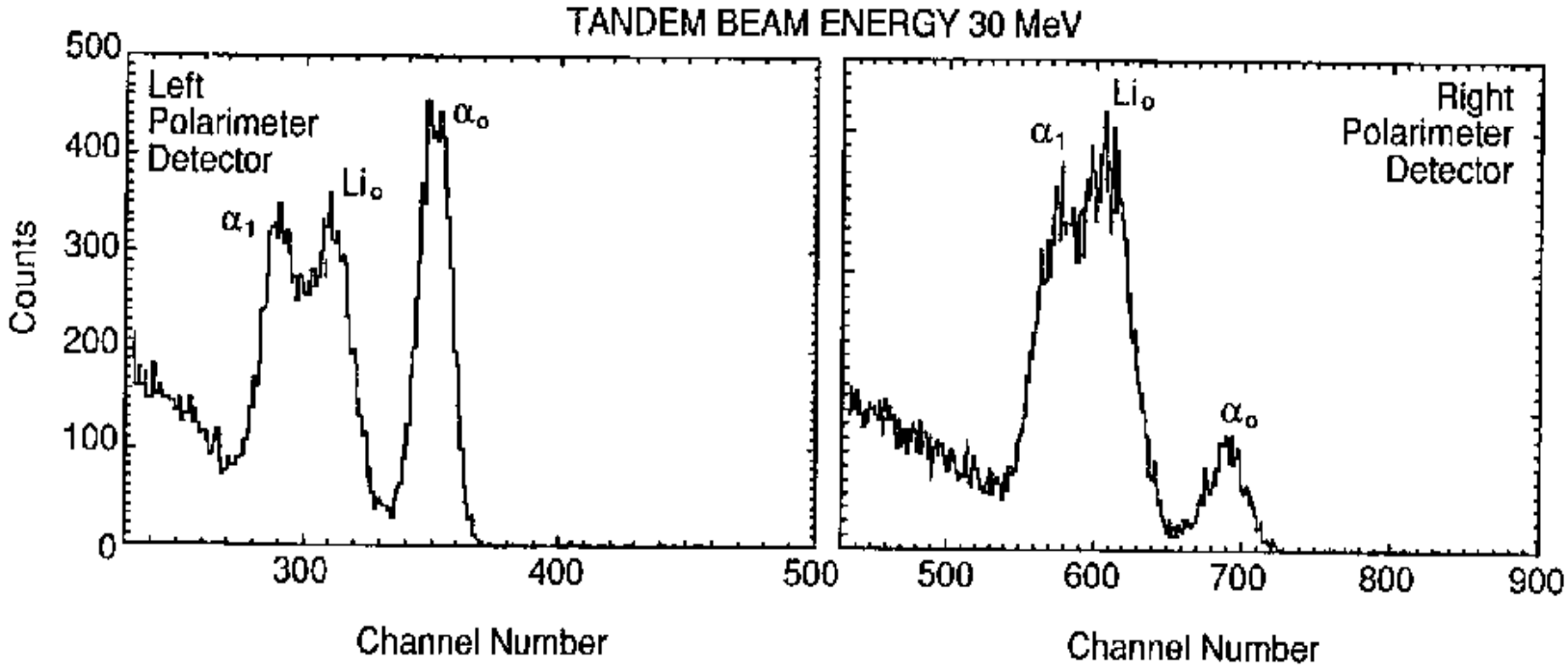

Scattering of $^{4}He(\vec{^{6}Li},^{6}Li)^{4}He$

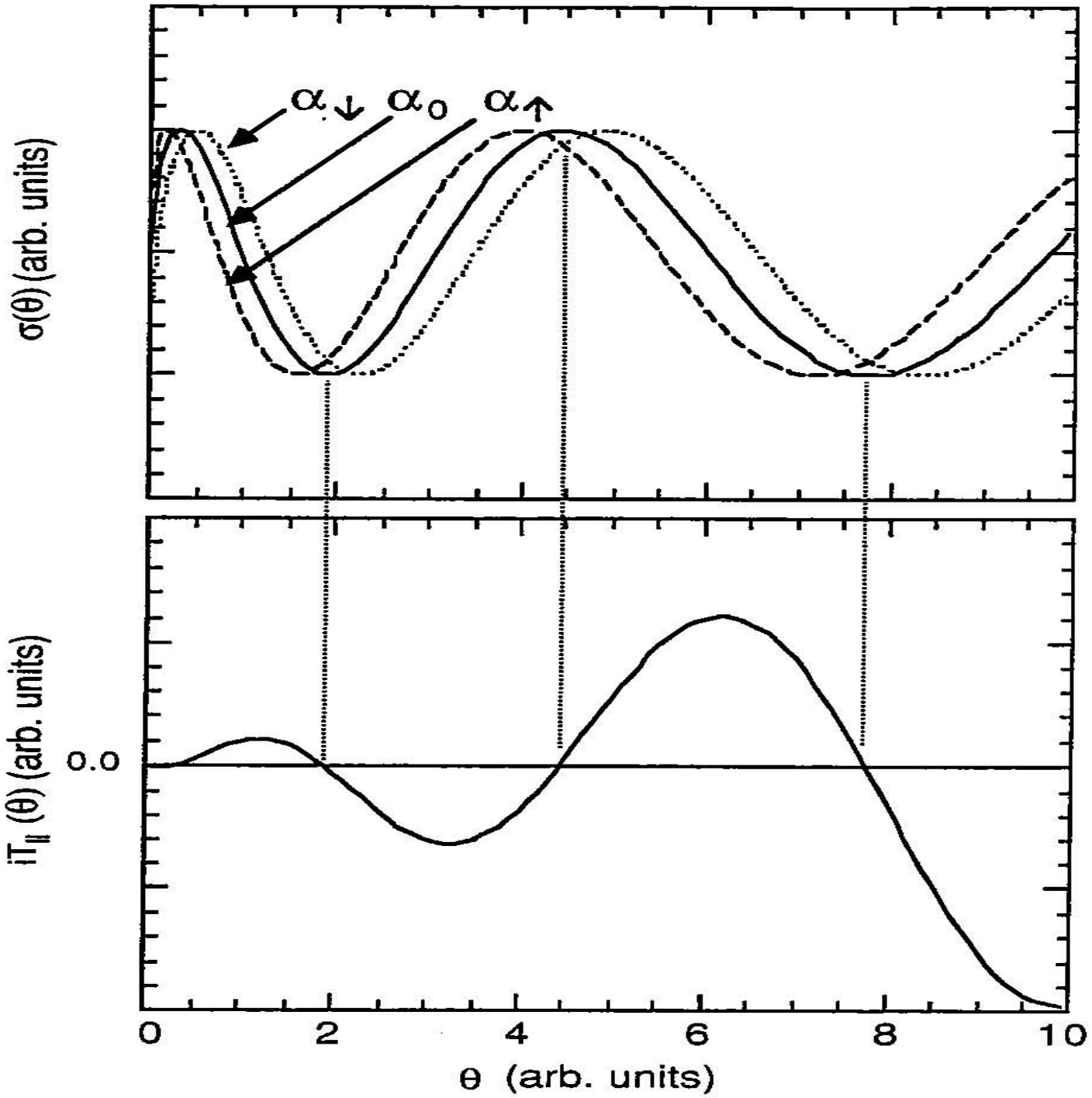
$\alpha_\downarrow$ α_0 $\alpha_\uparrow$
σ(θ) (arb. units)
$iT_{||}$ (θ) (arb. units)
0.0
0
2
4
6
8
10
θ (arb. units)

Phys Rev C82, 021602 (2010) Uesaka,et al

$\vec{p}$(6He, 6He)p

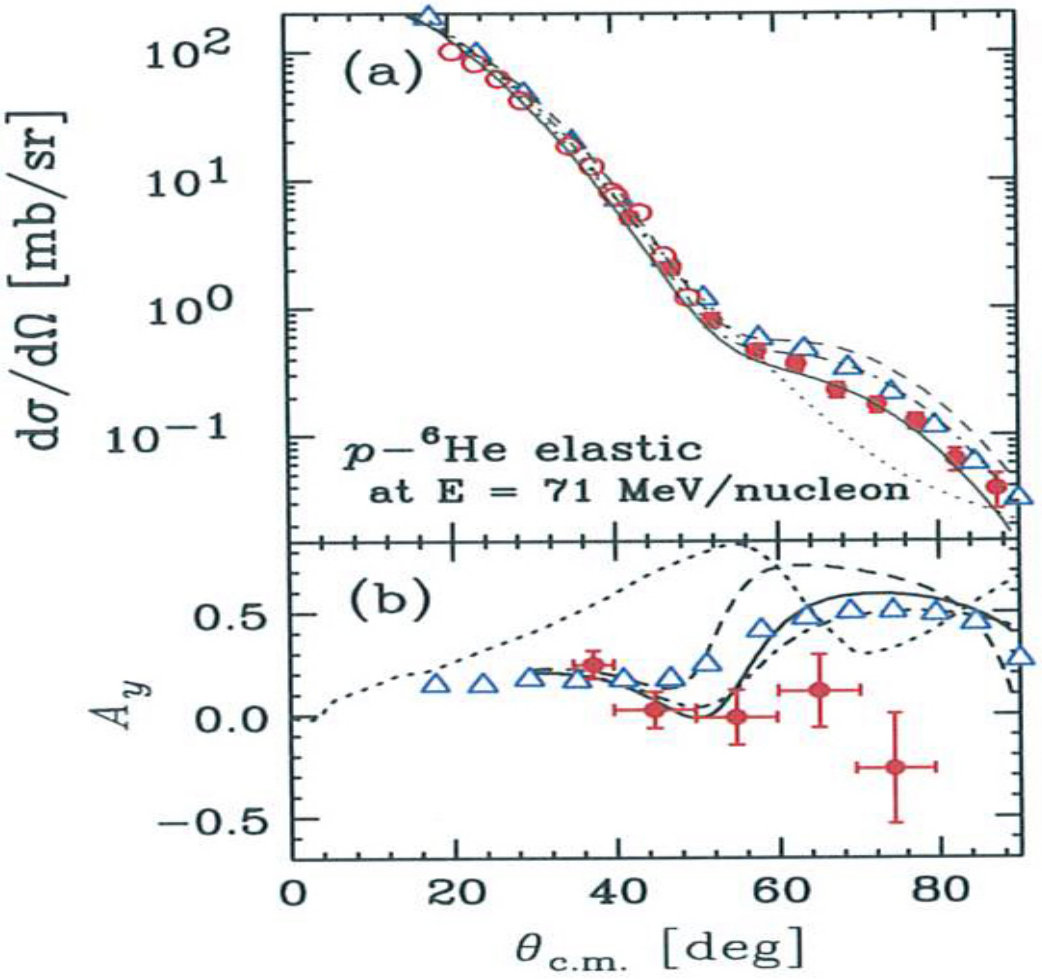

FIG. 2. (Color online) Cross section and vector analyzing power for the p-^{6}He elastic scattering at 71 MeV/nucleon (filled circles), together with cross-section data in Ref. [4] (open circles) and data for ^{6}Li [18] (triangles) targets. The dotted lines are a t-folding calculation in Ref. [20]. Results of 6BF calculations with harmonic oscillator (dashed), WS with (solid), and without halo (dot-dashed) single-particle wave functions are shown.

$^4He(\vec{p},p)^4He$ squares

$6He(\vec{p},p)6He$ Large Crosses

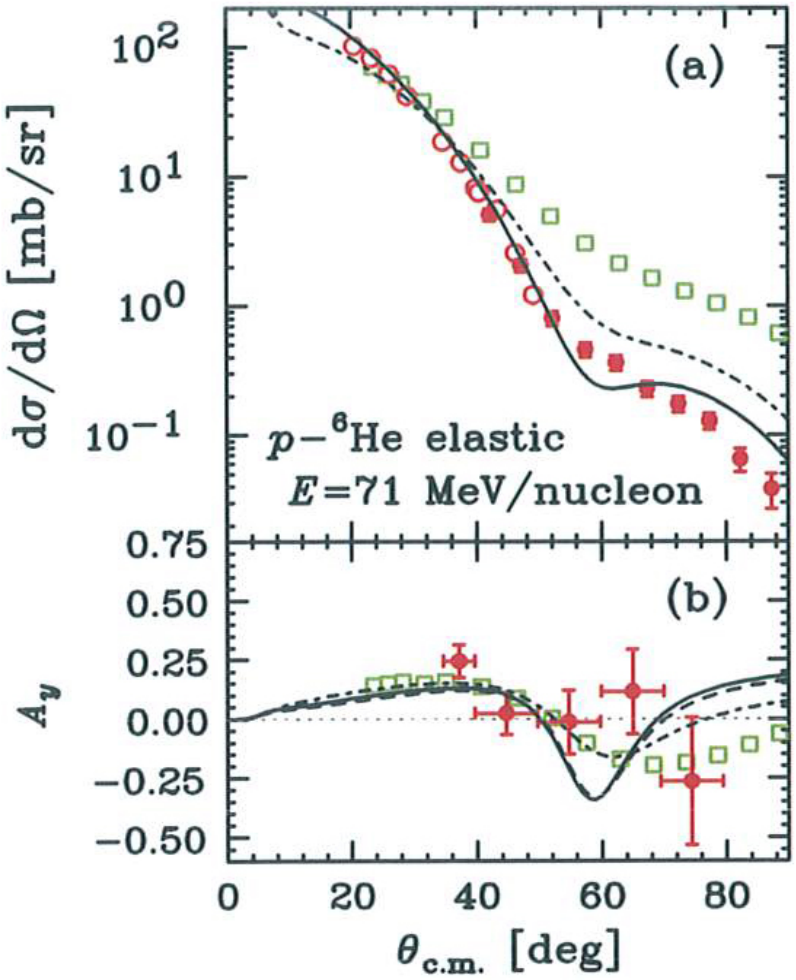

FIG. 3. (Color online) Present data compared with the cluster-folding calculations. Solid, dashed, and dot-dashed lines represent calculations with full, $V_{pn;\ell s} = 0$, and $V_{pn;\ell s} = V_{pn;\text{central}} = 0$ interactions, respectively. Data for the p-^{4}He scattering [22] (squares) are also shown.

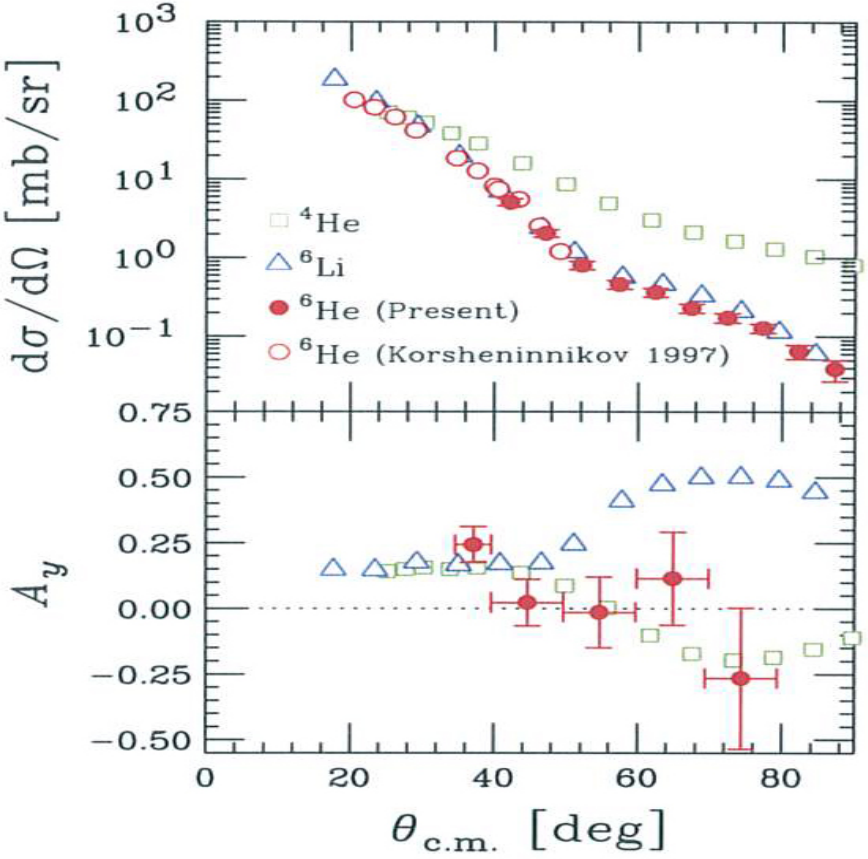

FIG. 7. (Color online) Differential cross sections and analyzing powers of p+^{4}He at 72 MeV (open squares: Ref. [23]), p+^{6}Li at 72 MeV (open triangles: Ref. [24]), and p+^{6}He at 71 MeV (open circles: Ref. [22]; closed circles: present work).

A_y of p+^{6}He decreases in $\theta_{c.m.} = 37°$–$55°$, which is rather similar to those of p+^{4}He. While the large error bars prevent us from observing the difference between A_y of p+^{6}He and of p+^{4}He, it is clearly seen that the angular distribution of A_y in p+^{6}He deviates from that of p+^{6}Li.

One last puzzle- what produces the spin of the proton? Called the spin crisis. Neat idea is you have 3 quarks each of Spin ½ they pair up and you are left with ½.

Do polarized electron scattering and get only one half of the spin. Propose rest of spin carried by the gluons. Polarized photons on polarized H and don't get required contribution to make ½.

Another puzzle you will work to solve

PR 93 (1954) 351

If this is done, one arrives at a problem that was solved ten years ago by Wannier,[3] and the resulting theory of susceptibility is essentially that already given by Dingle.[4]

[1] W. Band, Phys. Rev. 91, 249 (1953).
[2] R. Courant and D. Hilbert, *Methoden der Mathematischen Physik* (J. Springer, Berlin, 1931), second edition, Vol. I, Chap. 6, Sec. 4.
[3] G. H. Wannier, Phys. Rev. 64, 358 (1943).
[4] R. B. Dingle, Proc. Roy. Soc. (London) A212, 47 (1952).

The Density Effect for the Ionization Loss at Low Energies*

R. M. STERNHEIMER
Brookhaven National Laboratory, Upton, New York
(Received November 18, 1953)

THE density effect for the ionization loss of charged particles has been evaluated recently for a number of substances.[1] At low energies, the density effect is given by[1]

$$\Delta\frac{dE}{dx}=\frac{2\pi n_0 e^4}{mv^2}\sum_j f_j \ln\left(\frac{l_j^2}{\nu_j^2}\right), \tag{1}$$

where n_0 is the electronic density, f_j and ν_j are the oscillator strength and the atomic frequency [in units $\nu_p=(n_0e^2/\pi m)^{\frac{1}{2}}$] for the jth transition; l_j is given by

$$l_j=(\nu_j^2+f_j)^{\frac{1}{2}}. \tag{2}$$

In the experiment of Bakker and Segrè[2] on the stopping power for 340-Mev protons, this density effect was included, so that this experiment measures the ionization potential,[3]

$$I_{BS}=h\nu_p\prod_j l_j^{f_j}, \tag{3}$$

rather than the ionization potential for the isolated atom, $I=h\nu_p\Pi_j\nu_j^{f_j}$. When the values of I_{BS} are used to calculate the ionization loss, the density effect correction is given by

$$\delta=\sum_j f_j\ln\left(\frac{l_j^2+l^2}{\nu_j^2}\right)-l^2(1-\beta^2)-\sum_j f_j\ln\frac{l_j^2}{\nu_j^2}, \tag{4}$$

where l is determined by the equation:

$$\beta^{-2}-1=\sum_j f_j/(\nu_j^2+l^2). \tag{5}$$

The first two terms of (4) give the correction which would have to be applied if the atomic ionization potential were used [see Eq. (46) of A]. The last term is due to the density effect already included in I_{BS}. Equation (4) can be written

$$\delta=\sum_j f_j\ln\left(\frac{l_j^2+l^2}{l_j^2}\right)-l^2(1-\beta^2), \tag{6}$$

where the l_j are such that Eq. (3) is satisfied. This procedure was used in A to calculate δ and gives exact results for the case of solids. However, for gases the density effect at low energies is negligibly small so that the atomic ionization potential I should be used rather than I_{BS}. In A the values of the ionization potential for gases were obtained by interpolation of I_{BS} for neighboring substances in the periodic table. The correction $I_{BS}-I$ is very small. In view of (1) and (2), I/I_{BS} is given by $\exp(-D/2)$, where

$$D=\sum_j f_j\ln\left(1+\frac{f_j}{\nu_j^2}\right), \tag{7}$$

and $(2\pi n_0e^4/mv^2)D$ is the amount by which dE/dx for gases exceeds the value calculated using I_{BS}. D was calculated for some of the substances listed in Table I of A, using the ionization potentials and the f_j which are given in this table. The results are: $D(\mathrm{Li})=0.34$, $D(\mathrm{C})=0.22$, $D(\mathrm{Al})=0.056$, $D(\mathrm{Fe})=0.14$, $D(\mathrm{Cu})=0.13$, $D(\mathrm{Ag})=0.09$, $D(\mathrm{Sn})=0.05$, $D(\mathrm{W})=0.07$. By interpolation one finds: $D(\mathrm{N_2})=0.20$, $D(\mathrm{O_2})=0.17$, $D(\mathrm{Ne})=0.13$, $D(\mathrm{A})=0.09$, $D(\mathrm{Kr})=0.11$, $D(\mathrm{Xe})=0.05$.

It should be emphasized that these values of D are considerably uncertain because of the sensitivity of D to the distribution of the low frequencies ν_j which correspond to excitation of the outer electron shells. An alternative method of obtaining D is to deduce the effective ionization potential I_j of the outermost electron shell for the gas from the observed index of refraction n in the optical region,[4] which is given by:

$$n=1+\frac{f_j}{2[I_j/(h\nu_p)_{\mathrm{gas}}]^2}, \tag{8}$$

where $f_j=N_j/Z$ and N_j is the number of valence electrons which was taken as the number of electrons with the highest principal quantum number. Thus, for[4] Kr, $n=1.00043$, $f_j=8/36$, and $h\nu_p=0.085$ ry lead to $I_j=1.37$ ry. The density effect which would be measured for this dispersion oscillator in a solid is given by:

$$D=f_j\ln\left\{1+\frac{f_j}{[I_j/(h\nu_p)_{\mathrm{solid}}]^2}\right\}, \tag{9}$$

where $(h\nu_p)_{\mathrm{solid}}$ is the average of $h\nu_p$ for the neighboring solids measured by Bakker and Segrè.[2] Equation (9) gives: $D(\mathrm{N_2})=0.53$, $D(\mathrm{O_2})=0.48$, $D(\mathrm{Ne})=0.24$, $D(\mathrm{Kr})=0.26$, $D(\mathrm{Xe})=0.17$. A comparison of these values with those obtained above indicates the uncertainty in D. However, it should be noted that even with the larger values obtained from the index of refraction the correction is quite small. D may be compared with the square bracket of Eq. (11) of A for dE/dx which is $\sim$20. Thus, $D=0.5$ corresponds to $a\sim2.5$ percent increase of dE/dx. This correction is hardly outside the limits of error owing to the uncertainty of the experimental values[2,5] of I.

In view of the smallness of D and the uncertainty about its value, it seems questionable whether this correction should be applied at present to the ionization loss for gases.[6] For high energies ($p/\mu c\gtrsim100$) when the density effect for the gas is important, D is smaller than Eq. (7) and becomes zero when the ionization loss has attained saturation (dE/dx independent of I).

I would like to thank Dr. A. O. Hanson and Dr. G. N. Whyte for pointing out the existence of the correction for the ionization potential of gases.

* Work done under the auspices of the U. S. Atomic Energy Commission.
[1] R. M. Sternheimer, Phys. Rev. 88, 851 (1952). Unless otherwise indicated, we use here the same notation as in that paper, which will be referred to as A.
[2] C. J. Bakker and E. Segrè, Phys. Rev. 81, 489 (1951).
[3] Goldwasser, Mills, and Hanson, Phys. Rev. 88, 1137 (1952).
[4] H. H. Landolt and R. Bornstein, *Physikalisch-Chemische Tabellen* (Julius Springer, Berlin, 1923), fifth edition, Vol. 2, p. 961.
[5] R. Mather and E. Segrè, Phys. Rev. 84, 191 (1951); D. C. Sachs and J. R. Richardson, Phys. Rev. 89, 1163 (1953).
[6] We note that the Lorentz term and the damping effect (see reference 1) introduce additional corrections which may be of the same order as D.

Coulomb Excitation of Heavy and Medium Heavy Nuclei by Alpha Particles*

G. M. TEMMER AND N. P. HEYDENBURG
Department of Terrestrial Magnetism, Carnegie Institution of Washington, Washington, D. C.
(Received December 2, 1953)

WE wish to report some preliminary results concerning the Coulomb excitation of some 35 nuclei between $Z=20$ and $Z=90$ by both alpha particles and protons with energies up to 3.8 Mev. Recent work on this process induced by protons in tantalum, tungsten, and a few other heavy elements[1,2] has pointed up the great usefulness of this method in studying transition probabilities between low-lying nuclear energy levels. It seemed desirable to extend the scope of these investigations, especially since such very definite predictions are made concerning the properties of many of these excited states by the collective model of the nucleus.[3,4]

Because of their higher charge and lower velocity for a given energy, alpha particles are eminently suited for the electric excitation of nuclei of lower atomic number since the condition for the simplified classical treatment of the process,[5,6] $2Z_1Z_2e^2/\hbar v$

If this is done, one arrives at a problem that was solved ten years ago by Wannier,[2] and the resulting theory of susceptibility is essentially that already given by Dingle.[4]

[1] W. Band, Phys. Rev. 91, 249 (1953).
[2] R. Courant and D. Hilbert, *Methoden der Mathematischen Physik* (J. Springer, Berlin, 1931), second edition, Vol. I, Chap. 6, Sec. 4.
[3] G. H. Wannier, Phys. Rev. 64, 358 (1943).
[4] R. B. Dingle, Proc. Roy. Soc. (London) A212, 47 (1952).

The Density Effect for the Ionization Loss at Low Energies*

R. M. Sternheimer
Brookhaven National Laboratory, Upton, New York
(Received November 18, 1953)

THE density effect for the ionization loss of charged particles has been evaluated recently for a number of substances.[1] At low energies, the density effect is given by[1]

$$\Delta\frac{dE}{dx}=\frac{2\pi n e^4}{mv^2}\sum_j f_j \ln\left(\frac{l_j^2}{\nu_p^2}\right), \tag{1}$$

where n_0 is the electronic density, f_j and ν_j are the oscillator strength and the atomic frequency [in units $\nu_p\equiv(n_0e^2/\pi m)^{\frac{1}{2}}$] for the jth transition; l_j is given by

$$l_j=(\nu_j^2+f_j)^{\frac{1}{2}}. \tag{2}$$

In the experiment of Bakker and Segrè on the stopping power for 340-Mev protons, this density effect was included, so that this experiment measures the ionization potential,[3]

$$I_{BS}=h\nu_p\prod_j l_j^{f_j}, \tag{3}$$

rather than the ionization potential for the isolated atom, $I=h\nu_p\prod_j\nu_j^{f_j}$. When the values of I_{BS} are used to calculate the ionization loss, the density effect correction is given by

$$\delta=\sum_j f_j\ln\frac{(l_j^2+\beta^2)}{\nu_j^2}-\beta^2(1-\beta^2)-\sum_j f_j\ln\frac{l_j^2}{\nu_j^2}, \tag{4}$$

where I is determined by the equation:

$$\beta^2-1=\sum_j f_j/(\nu_j^2+\beta^2). \tag{5}$$

The first two terms of (4) give the correction which would have to be applied if the atomic ionization potential were used [see Eq. (46) of A]. The last term is due to the density effect already included in I_{BS}. Equation (4) can be written

$$\delta=\sum_j f_j\ln\frac{(l_j^2+\beta^2)}{l_j^2}-\beta^2(1-\beta^2), \tag{6}$$

where the l_j are such that Eq. (3) is satisfied. This procedure was used in A to calculate δ and gives exact results for the case of solids. However, for gases the density effect at low energies is negligibly small so that the atomic ionization potential I should be used rather than I_{BS}. In A the values of the ionization potential for gases were obtained by interpolation of I_{BS} for neighboring substances in the periodic table. The correction $I_{BS}-I$ is very small. In view of (1) and (2), I/I_{BS} is given by $\exp(-D/2)$, where

$$D=\sum_j f_j\ln\left(1+\frac{f_j}{\nu_j^2}\right), \tag{7}$$

and $(2\pi n_0e^4/m\nu_p^2)D$ is the amount by which dE/dx for gases exceeds the value calculated using I_{BS}. D was calculated for some of the substances listed in Table I of A, using the ionization potentials and the f_j which are given in this table. The results are: $D(\mathrm{Li})=0.34$, $D(\mathrm{C})=0.22$, $D(\mathrm{Al})=0.056$, $D(\mathrm{Fe})=0.14$, $D(\mathrm{Cu})=0.13$, $D(\mathrm{Ag})=0.09$, $D(\mathrm{Sn})=0.05$, $D(\mathrm{W})=0.07$. By interpolation one finds: $D(\mathrm{Na})=0.20$, $D(\mathrm{O}_2)=0.17$, $D(\mathrm{Ne})=0.13$, $D(\mathrm{A})=0.09$, $D(\mathrm{Kr})=0.11$, $D(\mathrm{Xe})=0.05$.

It should be emphasized that these values of D are considerably uncertain because of the sensitivity of D to the distribution of the low frequencies ν_j which correspond to excitation of the outer electron shells. An alternative method of obtaining D is to deduce the effective ionization potential I_j of the outermost electron shell for the gas from the observed index of refraction n in the optical region,[4] which is given by:

$$n=1+\frac{f_j}{2[I_j/(h\nu_p)_{\mathrm{gas}}]^2}, \tag{8}$$

where $f_j=N_j/Z$ and N_j is the number of valence electrons which was taken as the number of electrons with the highest principal quantum number. Thus, for* Kr, $n=1.00043$, $f_j=8/36$, and $h\nu_p=0.085$ ry lead to $I_j=1.37$ ry. The density effect which would be measured for this dispersion oscillator in a solid is given by:

$$D=f_j\ln\left\{1+\frac{f_j}{[I_j/(h\nu_p)_{\mathrm{solid}}]^2}\right\}, \tag{9}$$

where $(h\nu_p)_{\mathrm{solid}}$ is the average of $h\nu_p$ for the neighboring solids measured by Bakker and Segrè.[3] Equation (9) gives: $D(\mathrm{Ne})=0.53$, $D(\mathrm{O}_2)=0.48$, $D(\mathrm{Ne})=0.24$, $D(\mathrm{Kr})=0.26$, $D(\mathrm{Xe})=0.17$. A comparison of these values with those obtained above indicates the uncertainty in D. However, it should be noted that even with the larger values obtained from the index of refraction the correction is quite small. D may be compared with the square bracket of Eq. (11) of A for dE/dx which is ≈ 20. Thus, $D=0.5$ corresponds to a $\sim$2.5 percent increase of dE/dx. This correction is hardly outside the limits of error owing to the uncertainty of the experimental values[5,6] of I.

In view of the smallness of D and the uncertainty about its value, it seems questionable whether this correction should be applied at present to the ionization loss for gases.[6] For high energies ($p/\mu c\gtrsim 100$) when the density effect for the gas is important, D is smaller than Eq. (7) and becomes zero when the ionization loss has attained saturation (dE/dx independent of I).

I would like to thank Dr. A. O. Hanson and Dr. G. N. Whyte for pointing out the existence of the correction for the ionization potential of gases.

* Work done under the auspices of the U. S. Atomic Energy Commission.
[1] R. M. Sternheimer, Phys. Rev. 88, 851 (1952). Unless otherwise indicated, we use here the same notation as in that paper, which will be referred to as A.
[2] C. J. Bakker and E. Segrè, Phys. Rev. 81, 489 (1951).
[3] Goldwasser, Mills, and Hanson, Phys. Rev. 88, 1137 (1952).
[4] H. H. Landolt and R. Börnstein, *Physikalisch-Chemische Tabellen* (Julius Springer, Berlin, 1923), fifth edition, Vol. 2, p. 961.
[5] R. Mather and E. Segrè, Phys. Rev. 84, 191 (1951); D. C. Sachs and J. R. Richardson, Phys. Rev. 80, 1063 (1950).
[6] We note that the Lorentz term and the damping effect (see reference 1) introduce additional corrections which may be of the same order as D.

Coulomb Excitation of Heavy and Medium Heavy Nuclei by Alpha Particles*

G. M. Temmer and N. P. Heydenburg
Department of Terrestrial Magnetism, Carnegie Institution of Washington, Washington, D. C.
(Received December 2, 1953)

WE wish to report some preliminary results concerning the Coulomb excitation of some 35 nuclei between $Z=20$ and $Z=90$ by both alpha particles and protons with energies up to 3.8 Mev. Recent work on this process induced by protons in tantalum, tungsten, and a few other heavy elements[1,2] has pointed up the great usefulness of this method in studying transition probabilities between low-lying nuclear energy levels. It seemed desirable to extend the scope of these investigations, especially since such very definite predictions are made concerning the properties of many of these excited states by the collective model of the nucleus.[3,4]

Because of their higher charge and lower velocity for a given energy, alpha particles are eminently suited for the electric excitation of nuclei of lower atomic number since the condition for the simplified classical treatment of the process,[1,5] $2Z_1Z_2e^2/\hbar v \gg 1$ (Z_1 and Z_2 are the charges of projectile and target, v is their relative velocity), is well satisfied down to the lower end of the periodic table. A further advantage in the use of helium ions lies in the fact that they turn out to be relatively much less effective in exciting the troublesome characteristic K x-radiation as compared with the nuclear gamma radiation in the targets; for instance, at 3 Mev the relative yields of K x-rays and 137-kev gamma rays from tantalum are 2.27 for alpha particles and 14.8 for protons. Background problems are reduced by several orders of magnitude compared with proton excitation,[2] permitting us to operate with solid angles approaching 2π.

Our experimental set-up is very simple. The beam from our electrostatic generator strikes the target which is thick to the incident particles but thin to the emerging radiation. Either a 1-in. or 2-in. thick NaI(Tl) crystal (depending on the energy of the gamma radiation under study), separated from the target by about 0.040 in. aluminum and mounted on a Dumont 6292 photomultiplier tube, serves as the gamma-ray detector. This entire assembly is surrounded by a 1-in. layer of lead. The output is fed through a conventional linear amplifier to a single-channel pulse-height analyzer. A one-volt channel width is used throughout. The known gamma-ray lines of ionium (Th^{230}) at 68 kev and 142 kev, In^{115} at 190 kev, Cd^{111} at 170 kev and 247 kev, Na^{22} at 0.511 Mev (annihilation) and 1.28 Mev, and Cs^{281} at 662 kev are used for energy calibration of the system. We are able satisfactorily to detect radiation down to about 10 kev. Figure 1(a) shows the pulse-height distribution we obtain with a 5-mil tantalum target bombarded with 3-Mev alphas, exhibiting the K x-ray line at about 61 kev and the 137-kev gamma ray. Figure 1(b) gives a similar plot for a metallic 35-mil manganese target showing

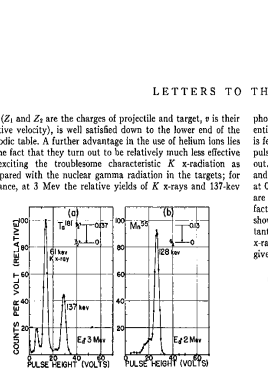

FIG. 1. (a) Pulse-height distribution of 137-kev gamma radiation and 61-kev K x-radiation from Ta^{181} bombarded by 3-Mev alphas. No absorber. (b) Pulse-height distribution of 128-kev gamma radiation from Mn^{55} bombarded by 2-Mev alphas. For previous level information, see reference 8.

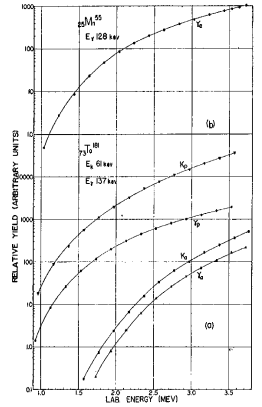

FIG. 2. (a) Excitation functions for K x-rays and gamma rays from Ta^{181}. $K_\alpha=K$ x-ray yield (protons); $\gamma_\alpha=137$-kev gamma-ray yield (protons); $K_\alpha-K$ x-ray yield (alphas); $\gamma_\alpha=137$-kev gamma-ray yield (alphas), γ_p and γ_α curves are *theoretical* thick target yield curves, normalized at the highest energy points. (b) Coulomb excitation of the 128-kev gamma ray from $_{25}\mathrm{Mn}^{55}$ by alpha particles. Solid curve is *theoretical* thick target yield curve, normalized at the highest energy. One-half the excitation energy has been subtracted before plotting experimental points in both (a) and (b).

TABLE I. Survey of levels below 500 kev observed by Coulomb excitation with 3-Mev alphas. Approximate intensity relative to Ta^{181} (*uncorrected* for relative abundance and internal conversion).

Element*	Abundance %	E_γ(observed) kev	Approx. int.	E_γ(known)[8] kev
$_{13}\mathrm{Al}^{27,3}$	92.5	478	···	478
$_{47}\mathrm{Ag}^{107,9}$	100	108, 196	···	110, 190
		1280	···	1280
$_{14}\mathrm{Na}^{28,6}$	100	430	···	440
$_{21}\mathrm{Sc}^{45}$	100	388	0.1	450
$_{73}\mathrm{Ta}^{181}$	7.8	155, 433	0.5, 0.08	185
$_{23}\mathrm{V}^{51}$	99.8	320	0.24	320
$_{25}\mathrm{Mn}^{55}$	100	128	10	130
$_{40}\mathrm{Zr}^{91}$	2.2	122	0.14	14, 117, 131
$_{50}\mathrm{Sn}^{121}$	4.1	93, 182	0.02, 0.06	92, 182
$_{32}\mathrm{Ge}^{74}$	7.7	68	0.33	54
$_{79}\mathrm{Au}^{197}$	100	68, 199, 283	0.02, 0.4, 0.3	67, 202, 281
$_{82}\mathrm{Se}^{77}$	7.6	(155), 237, 440	0.15, 0.2	160, 237
$_{72}\mathrm{Hf}^{180,177}$	72, 28	150	0.05	150, 410
$_{82}\mathrm{Se}^{82}$	··	360	0.07	?
$_{42}\mathrm{Zr}^{94}$	1.5†	900†	0.14	80, 934
$(_{72}\mathrm{Hf}^{178,180})$				
$_{48}\mathrm{Mo}^{98}$	15.7	198	0.05	200
$_{45}\mathrm{Rh}^{103}$	100	305, 370	0.1, 0.04	40
$_{46}\mathrm{Pd}^{105}$	22.6	687	0.02	63
$_{48}\mathrm{Cd}^{111}$	12.8	300?	0.01	247, 340
$_{49}\mathrm{In}^{115}$	95.8	500	···	500‡
$_{51}\mathrm{Sb}^{123}$	42.8	~160	0.02	153
$_{58}\mathrm{Ce}^{136}$	100	85	0.6	81
$_{39}\mathrm{Y}^{89}$	100	~150	0.01	145
$_{62}\mathrm{Sm}^{150}$	26.6	119	2.5	122
$_{71}\mathrm{Yb}^{176}$	3.0	82	0.6	84
$_{74}\mathrm{Ta}^{186}$	100	137	1.00	137
$_{74}\mathrm{W}^{180,182,184}$	85.4	~120	1.3	102, 113, 124†
$_{81}\mathrm{Tl}^{205}$	29.5	220?	0.003	270
$_{90}\mathrm{Th}^{232}$	100	50	0.20	50

* The following elements did not show lines below 500 kev with alphas: Mg, Al, Si, P, S, Cl, K, Ca, Cr, Co, Ni, Cu, Ga, Nb, Ag, Te, Pt, Au, Pb, Bi.
† See reference 9.
‡ Via compound nucleus. For $Z<20$ see text.
# All entries refer to 1H isotopic (3%).
+ With protons only.

[1] T. Huus and J. H. Bjerregaard, Phys. Rev. 92, 1579 (1953).

nature of the excitation process down to at least $Z=25$ for alphas and up to 3.6 Mev for protons on tantalum ($Z=73$). We postpone a detailed discussion of the results on the various nuclei we have investigated and restrict ourselves to a tabular presentation of the salient features in Table I. We list, in turn, the target nucleus, mass number, and relative abundance of the isotope believed responsible for the radiation, gamma-ray energy observed and energy levels known from other sources,[8] and a qualitative estimate of the relative yield of the observed radiation under 3-Mev alpha bombardment, *uncorrected* for internal conversion. The highest line excited was at 500 kev (In^{115}).

Elements with $Z<20$ are included here mainly for the purpose of demonstrating the main sources of radiation from possible light-element impurities. Li, F, and Na are found to be the only light elements yielding gamma rays below 500 kev under alpha bombardment. The excitations of the 478-kev state in Li^7 and the first two excited states in F^{19} at 108 kev and 196 kev (mainly by ordinary interlastic scattering of alphas involving compound nucleus formation with sharp resonances) have been studied and will be the subject of another publication.[10] In this connection, we have found striking evidence for Coulomb excitation of the 196-kev level in fluorine (second excited state) by alphas below 2.2 Mev before the onset of the resonances. This phenomenon is not observable with protons because of the complicated resonance structure which then extends down to very low energies.

We are extending our measurements into the rare-earth region where many nuclei have low-lying excited states. Our final results will include determinations of absolute yields and hence values of the reduced transition probabilities $B_\gamma(2)$,[5] as well as a comparison of the experimental facts with the rotational interpretation[8,4] of these levels.

* A preliminary account of this work will be presented at the New York meeting of the American Physical Society, January 28–30, 1954.
[1] T. Huus and C. Zupancič, Kgl. Danske Videnskab. Selskab, Mat.-fys. Medd. 28, No. 1 (1953).
[2] C. McClelland and C. Goodman, Phys. Rev. 91, 760 (1953).
[3] A. Bohr and B. R. Mottelson, Kgl. Danske Videnskab. Selskab. Mat.-fys. Medd. 27, No. 16 (1953).
[4] D. Hill and J. A. Wheeler, Phys. Rev. 89, 1102 (1953).
[5] K. A. Ter-Martirosyan, J. Exptl. Theor. Phys. (U.S.S.R.) 22, 284 (1952).
[6] K. Alder and A. Winther, Phys. Rev. 91, 1578 (1953).
[7] We observe (capture) gamma radiation with energies greater than 4 Mev from most medium-heavy nuclei under proton bombardment.
[8] This level is known only from $\mathrm{Mo}^{98}(p,p')\mathrm{Mo}^{98}$, see Hausman, Allen, Arthur, Bender, and McDole, Phys. Rev. 88, 1296 (1951).
[9] Mostly as collected in Way, Fano, Scott, and Thew, *Nuclear Data*, National Bureau of Standards Circular 499 (U. S. Government Printing Office, Washington, D. C., 1950) and supplements; and Hollander, Perlman, and Seaborg, Revs. Modern Phys. 25, 469 (1953).
[10] N. P. Heydenburg and G. M. Temmer, Phys. Rev. (to be published); a preliminary account will be presented at the New York meeting of the American Physical Society, January 28–30, 1954.

The Specific Ionization and Energy Loss of a Fast Charged Particle

J. R. Allen*
H. H. Wills Physical Laboratory, Bristol, England
(Received October 19, 1953)

IT may be shown that the primary ionization and excitation density j_P (i.e., the average number of electrons excited or ejected per unit volume either directly or by absorption of Čerenkov radiation), because of the passage of a fast charged particle through a medium, is, at distances greater than ρ_0, the minimum impact parameter, given by

$$j_P=\frac{c}{\beta}\int_{\omega_0}^{\infty}\Phi\frac{\mathfrak{G}}{\omega}\,d\omega. \tag{1}$$

In this equation, the particle's field is treated as a perturbation in a semiclassical approximation; $\epsilon(\omega)$ is the photoelectric absorption coefficient; $\mathfrak{G}(\omega,\rho)$ is the Fourier time transform of the effective electric field.

If $\mathfrak{G}$ is calculated by the phenomenological approximation due to Fermi,[1] Eq. (1) and the similarly derived equation for the energy absorption density may be integrated over all impact parameters greater than ρ_0. We obtain for the total primary ionization and excitation ($\rho>\rho_0$)

$$P(\rho_0)=\int\Phi dE,\quad \tau\neq 0;\quad P=0,\quad \tau=0 \tag{2}$$

and for the total energy absorption ($\rho>\rho_0$)

$$\Gamma\tau(\rho_0)=W_\tau\int\Phi E dE,\quad \tau\neq 0;\quad \Gamma\tau=0,\quad \tau=0, \tag{3}$$

where

$$\Phi=\frac{\alpha^2Z^2}{\pi a_0\beta^2}\frac{\delta}{\kappa^2\zeta}\,\mathrm{Im}[\zeta^2K_0^2(\xi)K_1(\zeta)];$$

$\kappa=\epsilon'+i\epsilon''$ is the complex dielectric constant; $\xi=(\eta^2+\beta^2)^{\frac{1}{2}}$; $\eta=1-\beta^2\epsilon'$, $\zeta=\beta^2\epsilon''$; $\zeta=[\omega_0\rho/2\sqrt{2}a_0\beta]\sqrt{(\xi+\eta)}-i\sqrt{(\xi-\eta)}$; W_τ is the Rydberg energy; a_0 is the Bohr radius; and E_τ the energy of the field components, is in rydbergs. Equation (3) is equivalent to Fermi's formula (22)[1] when $\tau\neq 0$.

The absorption coefficient τ and the dielectric constant ϵ' were obtained for silver bromide by the methods described below and Eqs. (2) and (3) were integrated numerically for all transfers less than 5000 ev. The results relative to the plateau values are shown in Fig. 1 plotted against the kinetic energy of the particle in units of mc^2. A discussion of the absorption resulting from the valence band of silver bromide has already been published,[2] and it was shown that the large polarizability of this salt results in a considerable modification in the shape of the absorption bands. Also, partly because of the large polarizability and partly because of the effect of the exclusion principle, there is a shift in the oscillator strengths towards the lower frequency bands. These considerations have been extended to the calculation of the absorption from the next few bands lying below the valence levels. The shape of the absorption curves being assumed to be in accordance with these calculations, their magnitudes were checked by a comparison of the computed with the empirically observed dispersion in the visible and ultraviolet. The oscillator strengths and absorption coefficients for the far x-ray region were taken from experimental values,[3,4] whereas for intermediate frequencies the absorption was calculated by the methods of Stobbe[5] using appropriate screening constants and a correction for the polarization effect near the absorption edge. The values of the absorption edges (in Rydberg units) and the total oscillator strengths for the various bands are shown in Table I. The dielectric constant was computed from the absorption coefficient.

These detailed expressions for τ and ϵ' change considerably the conclusions obtained when a simple line absorption model is used, and the oscillator strengths are assumed proportional to the

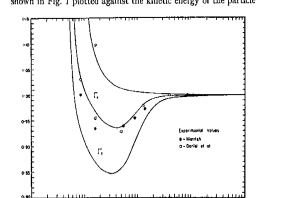

FIG. 1. F, the primary ionization and excitation; $\Gamma\tau$, the energy absorption; and $T\tau$, the kinetic energy of the primary electron: computed for a singly charged particle (transfers <5000 ev, distances >2a) and shown relative to the plateau values $F(\beta=1)=50\,690/\mathrm{cm}$, $\Gamma\tau(\beta=1)=3.31$ Mev/cm, $T\tau(\beta=1)=1.21$ Mev/cm as functions of E/mc^2 (E=kinetic energy). Experimental values of relative grain density are due to Daniel *et al.* (reference 8) (marked ○) and Morrish (reference 9) (marked ●).

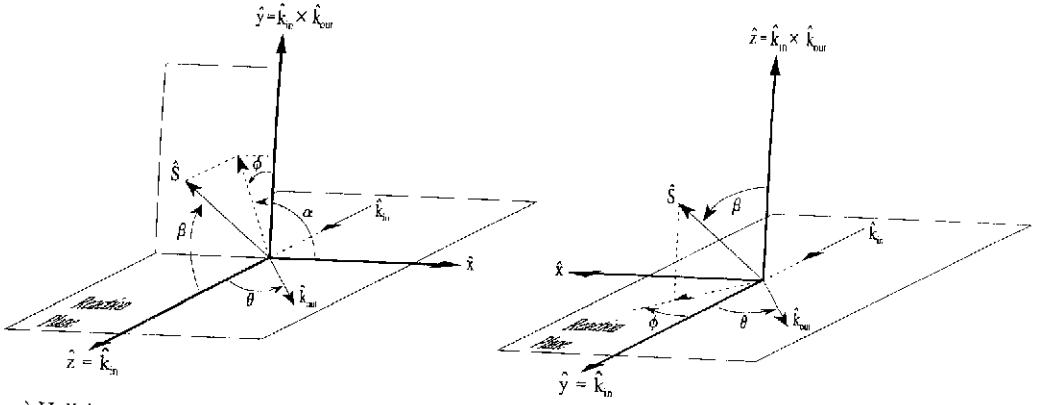

a) Helicity frame.

b) Transverse frame.

Figure A.1 Two coordinate systems commonly used for describing polarization observables.

APPENDIX A

PROPERTIES OF POLARIZATION OBSERVABLES

This appendix summarizes the properties of spin tensor moments and analyzing powers. The formulae can be found in [Sim74], unless otherwise noted. The coordinate systems used are shown in fig. A.1, and the polarization observables are as defined in the Madison convention [BH71].

The spin tensor moments, also called (irreducible) statistical tensors, are defined in terms of the spin density matrix elements:

$$t_{kq} \equiv \sum_{mm'} \hat{I}\hat{k}(-)^{I-m-q} \begin{pmatrix} I & I & k \\ m' & -m & -q \end{pmatrix} \rho_{m'm} \qquad \text{(A.1)}$$

The Wigner 3-j symbol is as defined by Brink and Satchler [BS62], and $\hat{k} \equiv \sqrt{2k+1}$. Analyzing powers are defined by the following expression for the polarized differential cross section

$$\left[\frac{d\sigma}{d\Omega}\right]_{pol} = \left[\frac{d\sigma}{d\Omega}\right]_{unpol} \times \sum_{kq} t_{kq} \cdot T^*_{kq} \qquad \text{(A.2)}$$

The analyzing powers in a reaction a + b $\rightarrow$ c + d can be related to the quantum mechanical scattering amplitudes $F^{\alpha\beta}_{\gamma\delta}$ as expressed in

$$T_{kq}(a) = \frac{\sum_{\alpha\alpha'\beta\gamma\delta} \hat{I}_a \hat{k} (-)^{I_a - \alpha - q} \begin{pmatrix} I_a & I_a & k \\ \alpha' & -\alpha & -q \end{pmatrix} \left(F_{\gamma\delta}^{\alpha\beta}\right)^* F_{\gamma\delta}^{\alpha'\beta}}{\sum_{\alpha\beta\gamma\delta} \left|F_{\gamma\delta}^{\alpha\beta}\right|^2} \qquad \text{(A.3)}$$

where α, β, γ, δ are the magnetic quantum numbers associated with the intrinsic spins $I_{a,b,c,d}$ of the particles a, b, c, d. The t_{kq} and T_{kq} are Hermitian, and so both obey $t_{kq}^* = (-)^q t_{k\,-q}$. Since both t_{kq} and T_{kq} are components of spherical tensors, their rotation properties are given by equations (A.4),

$$\begin{aligned} &\text{(a)} \quad t_{kq}^{II} = \sum_{q'} D_{q'q}^{k}(\alpha\beta\gamma)\, t_{kq'}^{I} \\ &\text{(b)} \quad t_{kq}^{I} = \sum_{q'} D_{qq'}^{k\,*}(\alpha\beta\gamma)\, t_{kq'}^{II} \\ &\text{(c)} \quad t_{kq}^{\ \prime} = \sum_{q'} D_{qq'}^{k\,*}(\alpha\beta\gamma)\, t_{kq'} \end{aligned} \qquad \text{(A.4)}$$

in which (a) & (b) describe the same state in two frames connected by rotation through Euler angles α, β & γ, and (c) connects rotated states in the same frame.

The preceding formulae are general; the following refer to one of two special coordinate systems, either the helicity (H) frame in the Madison convention [BH71], or the transverse (T) frame, both shown previously in fig. A.1. Throughout this discussion transverse equations will have T superscripted analyzing powers, and helicity equations will be unsuperscripted.

If the existence of a spin symmetry axis is a good approximation, then the tensor moments are zero for $q \neq 0$ in a coordinate system where the z-axis is parallel to the

symmetry axis. Tensor moments in this coordinate system will be denoted $\hat{t}_{k0}$. The tensor moments in the helicity frame can be written in term of these $\hat{t}_{k0}$ by applying equation (A.4b),

$$t_{kq} = D^{k*}_{q0}(\alpha,\beta,0)\,\hat{t}_{k0} = \sqrt{\tfrac{4\pi}{2k+1}}\,Y_{kq}(\beta,\alpha)\,\hat{t}_{k0}. \qquad (A.5)$$

Historically, the angle $\phi = \alpha - \pi/2$ (see fig. A.1) has been used rather than the more conventional Euler angle α to describe the orientation of the spin symmetry axis in the H frame. Equation (A.6) has been written in terms of ϕ and β.

If parity conserving reactions are used, then $T_{kq} = (-)^{k-q}\,T_{k-q}$ and ${}^{r}T_{kq} = (-)^{q}\,{}^{r}T_{kq}$, and likewise for the t_{kq}. Hermiticity and parity conservation, together with (A.5), can be used to obtain from (A.2) the following explicit expression for the polarized differential cross section in the H frame:

$$\frac{\left(\frac{d\sigma}{d\Omega}\right)_P}{\left(\frac{d\sigma}{d\Omega}\right)_u} = \{1 + \sqrt{2}\sin\beta\cos\phi\,\hat{t}_{10}iT_{11} + \tfrac{1}{2}(3\cos^2\beta - 1)\hat{t}_{20}T_{20}$$
$$+ \sqrt{6}\sin\beta\cos\beta\sin\phi\,\hat{t}_{20}T_{21} - \sqrt{\tfrac{3}{2}}\sin^2\beta\cos2\phi\,\hat{t}_{20}T_{22} \qquad (A.6)$$
$$- \sqrt{\tfrac{5}{4}}\sin^3\beta\cos3\phi\,\hat{t}_{30}iT_{33} + \sqrt{\tfrac{17}{2}}\sin^2\beta\cos\beta\sin2\phi\,\hat{t}_{30}iT_{32}$$
$$+ \sqrt{\tfrac{3}{4}}\sin\beta(5\cos^2\beta - 1)\cos\phi\,\hat{t}_{30}iT_{31}\}.$$

The connection between H frame and T frame analyzing powers is given by the following equations (the cartesian AP are defined in the H frame):

$$^{T}T_{10} = \sqrt{2}\, iT_{11} = \sqrt{\frac{3}{2}}\, A_{y} = \text{purely real.} \tag{A.7}$$

$$^{T}T_{20} = -\frac{1}{2}\, T_{20} - \sqrt{\frac{3}{2}}\, T_{22} = \sqrt{\frac{1}{2}} A_{yy} = \text{purely real.} \tag{A.8}$$

$$^{T}T_{22} = -\sqrt{\frac{3}{8}}\, T_{20} + iT_{21} + \frac{1}{2}\, T_{22} = \text{complex.} \tag{A.9}$$

$$^{T}T_{30} = -\sqrt{\frac{3}{4}}\, iT_{31} - \sqrt{\frac{5}{4}}\, iT_{33} = \text{purely real.} \tag{A.10}$$

$$^{T}T_{32} = -\sqrt{\frac{5}{8}}\, iT_{31} - T_{32} + \sqrt{\frac{3}{8}}\, iT_{33} = \text{complex.} \tag{A.11}$$

Additionally, the following cartesian AP are sometimes used:

$$A_{xx} = \sqrt{3}\, T_{22} - \sqrt{\frac{1}{2}}\, T_{20} = \text{purely real.} \tag{A.12}$$

$$A_{zz} = \sqrt{2}\, T_{20} = \text{purely real.} \tag{A.13}$$

$$A_{xz} = -\sqrt{3}\, T_{21} = \text{purely real.} \tag{A.14}$$

Note that the above definitions imply

$$A_{xx} + A_{yy} + A_{zz} = 0. \tag{A.15}$$